Lemoni *et al.*
Biotechnology for the Environment (2026) 3:5
https://doi.org/10.1186/s44314-026-00039-8

Biotechnology for the Environment

RESEARCH

Open Access

Process optimization and predictive modeling of multi-enzyme extraction of bioactive compounds from *Rosa canina* L.

Zafeiria Lemoni[1], Georgia Theodoreli[1], Styliani Kalantzi[1], Theopisti Lymperopoulou[2], Andromachi Tzani[3], Georgios Stavropoulos[4], Anastasia Detsi[3] and Diomi Mamma[1*]

Abstract

The pseudo-fruit of *Rosa canina* L. represents a valuable resource of bioactive compounds known for their antioxidant, anti-inflammatory, antimicrobial, anti-diabetic, anti-aging, and anticancer properties. In this work, the enzyme-assisted extraction (EAE) of bioactive compounds from pseudo-fruit of *Rosa canina* L. was developed and optimized using four hydrolytic enzyme preparations: cellulolytic (Cellic® CTec3 HS), pectinolytic (Pectinex® Ultra Color), hemicellulolytic (Viscoferm®), and proteolytic (Neutrase®). A six-factor Box–Behnken Design (BBD) was employed to systematically evaluate the effects of enzyme loadings-Cellic® CTec3 (0.1–0.3% v/v), Pectinex® Ultra Color (0.1–0.3% v/v), Viscoferm® (0.2–0.6% v/v), and Neutrase® (0.1–0.2% v/v)-as well as agitation speed (300–1300 rpm) and extraction time (60–120 min) on the overall process. The extracts were characterized in terms of their performance in total phenolic compounds (TPC) by the Folin Ciocalteu method, in total flavonoid content (TFC) by the aluminum chloride colorimetric method, and in antioxidant activity by the DPPH free radical scavenging capacity. The optimum extract was evaluated for its biological activities, anti-aging (inhibition of tyrosinase activity), antidiabetic (inhibition of α-amylase activity), and antibacterial activity against *Escherichia coli*. The optimal conditions were determined by the Derringer desirability function for 0.1%v/v Cellic® CTec3 HS, 0.1%v/v Pectinex® Ultra Color, 0.21%v/v Viscoferm®, and 0.12%v/v Neutrase® at 782 rpm stirring speed and 60 min extraction time. The optimum extract yielded TPC of 122.1 ± 3.58 mg GAE/g DW, TFC of 47.3 ± 2.0 mg CAE/g DW, and antioxidant activity with an IC_{50} of 0.72 ± 0.07 $\mu L_{extract}$/mL. A control experiment was carried out under identical conditions without enzyme addition and achieved TPC of 41.6 ± 1.8 mg GAE/g DW and TFC of 20.9 ± 1.2 mg CAE/g DW. The biological activities of the extracts revealed strong inhibition of *E. coli* growth, moderate tyrosinase inhibition, and weak α-amylase inhibition. Sustainability of the extraction method was confirmed through AGREEprep, a green analysis tool, in accordance with green analytical chemistry principles. This study highlights a fast and efficient multi-enzyme approach for extracting bioactive compounds from *Rosa canina* L. pseudofruit, yielding extracts with potential applicability across diverse industrial sectors, such as in cosmetology and in nutraceuticals.

Keywords Enzyme-assisted extraction (EAE), Rosa canina L., Box–Behnken Design (BBD), Bioactive compounds, Optimization, Modeling, Biological activities, AGREEprep

*Correspondence:
Diomi Mamma
dmamma@chemeng.ntua.gr
Full list of author information is available at the end of the article

© The Author(s) 2026. **Open Access** This article is licensed under a Creative Commons Attribution 4.0 International License, which permits use, sharing, adaptation, distribution and reproduction in any medium or format, as long as you give appropriate credit to the original author(s) and the source, provide a link to the Creative Commons licence, and indicate if changes were made. The images or other third party material in this article are included in the article's Creative Commons licence, unless indicated otherwise in a credit line to the material. If material is not included in the article's Creative Commons licence and your intended use is not permitted by statutory regulation or exceeds the permitted use, you will need to obtain permission directly from the copyright holder. To view a copy of this licence, visit http://creativecommons.org/licenses/by/4.0/.

Introduction

The industrial utilization of plant-derived bioactive compounds is frequently limited by inefficient extraction processes that require extended processing times and energy-demanding conditions, affecting the economic feasibility of the overall process. Consequently, there is increasing interest in extraction strategies that simultaneously improve yield and limit environmental burden. In parallel, the growing consumer demand for safe, sustainable, and environmentally friendly products has intensified the development of greener extraction [1–3]. Enzyme-assisted extraction (EAE) has emerged as a promising method to address these challenges, leveraging the inherent ability of enzymes to selectively degrade plant matrices efficiently [4], while aligning with the principles of green chemistry and circular bioeconomy [4–6]. Hydrolytic enzymes selectively degrade the most abundant structural polysaccharides in the plant matrices along with protein networks, facilitating the release of intracellular compounds [7]. Although the potential of EAE has been demonstrated in a variety of plant species, the optimization of such processes remains complex due to the multiple interacting variables that affect enzyme performance, such as enzyme loading, agitation speed, temperature, and extraction time [4, 8, 9]. Statistical design of experiments provides a systematic framework for exploring complex parameter spaces and identifying optimal conditions with reduced experimental effort. In particular, response surface methodology (RSM) enables the evaluation of both individual factor effects and interactions between variables. The Box–Behnken Design (BBD) offers an efficient experimental layout that is especially suitable for enzymatic systems involving multiple interdependent factors [10, 11].

Rosa canina L. is a wild species widely distributed in Europe and known for its remarkable content of polyphenols and therefore its biological activities, such as antioxidant, antimicrobial, antiaging, and antidiabetic [12–14]. However, despite extensive literature on the phytochemical composition of *Rosa canina* L., the implementation of multi-enzymatic extraction strategies and their predictive modeling remains limited [15–17].

Several green analysis tools have been developed in the past years, based on the Green Analytical Chemistry (GAC) concept and Green Sample Preparation (GSP), to assess the sustainability and effectiveness of the aforementioned processes, such as Analytical Eco-Scale, GAPI (Green Analytical Procedure Index), and NEMI (National Environmental Methods Index) [18–20]. GAC is a framework inspired by the 12 Principles of Green Chemistry, while focusing on reducing waste generation, sample and solvent consumption, and energy use [21, 22]. GSP was subsequently introduced to minimize and eliminate hazardous solvents and energy-intensive processes by promoting safer, more sustainable alternatives [23]. AGREEprep (Analytical Greenness Metric for Sample Preparation) is one of the recent tools that quantifies the greenness and sustainability of analytical processes and presents the results through color-coded pictograms [24].

The present study addresses these challenges by developing a multi-enzyme-assisted extraction strategy of bioactive compounds from *Rosa canina* L. pseudofruit and systematically optimizing key process parameters using a BBD. The extraction efficiency was evaluated through chemical and biological indicators, while predictive models were established to describe the relationships between process parameters and responses. In parallel, the environmental performance of the extraction process was assessed using AGREEprep, offering an integrated perspective on efficiency and sustainability.

Materials and methods

Plant material

Rosa canina L. pseudofruit was processed as previously described in earlier studies [16]. Briefly, dried rosehips were supplied by Korres S.A.-Natural Products and originated from plants cultivated and preserved at the Balkan Botanic Garden of Kroussia, located in northern Greece, near the mountain village of Pontokerasia in the Kilkis Regional Unit (coordinates: 41°05′ N 23°06′ E). The pseudofruits were harvested in the first days of October. Following manual deseeding, the dried rosehips were milled to an average particle size of < 500 μm using an Electric Grain Mill Grinder (HC-550, VEVOR, China). The resulting powdered material was stored in sealed plastic containers at room temperature until further use.

Chemicals and reagents

The reagents employed—2,2-Diphenyl-1-picrylhydrazyl ($DPPH^{\cdot}$), absolute methanol (CH3OH), and Folin–Ciocalteu—were purchased from Sigma-Aldrich (St. Louis, MO, USA). All additional chemicals were of analytical grade and obtained from Sigma Chemical Co. (St. Louis, MO, USA).

Enzyme preparations

The commercial enzyme preparations used in this study were multi-enzyme mixtures. The enzymatic activities were experimentally determined and expressed as Units/mL (U/mL). The measured activities were as follows: Neutrase® (protease activity, 5 U/mL), Pectinex® Ultra Color (polygalacturonase activity, 95 U/mL), Viscoferm® (xylanase activity, 4500 U/mL), and Cellic® CTec3 HS (total cellulolytic activity, 120 FPU/mL). All enzyme preparations were kindly provided by Novozymes A/S (Bagsværd, Denmark). Tyrosinase (EC 1.14.1.8.1) from

mushroom and α-amylase from porcine pancreas were purchased from Sigma-Aldrich (St. Louis, MO, USA).

Experimental design and response surface methodology

The process optimization was carried out using a response surface methodology (RSM) approach, as previously applied in related studies [17]. A six-factor Box–Behnken Design (BBD) was employed to evaluate the combined effects of enzyme loadings, agitation speed, and extraction time on the response variables, namely total phenolic content (TPC), total flavonoid content (TFC), and antioxidant activity. The independent variables and their corresponding levels are presented in Table 1, while the complete experimental matrix of the BBD along with the measured response values is shown in Table 2. The design comprised 54 experimental runs, including six center points, and the selected variable ranges were established based on preliminary experiments. Quadratic polynomial models were developed to describe the relationships between the independent variables and the response parameters.

Enzyme-assisted extraction

Enzyme-assisted extraction experiments were performed following the procedure previously described in our earlier publications [16]. Briefly, the milled plant material was suspended in 50 mM phosphate buffer (pH 6) at a fixed solid-to-liquid ratio (6% w/v), and treated with the appropriate enzyme combinations as defined by the BBD. Enzyme loading (% v/v) was defined as the volume of liquid enzyme preparation relative to the total volume of the solvent–buffer system. The enzyme was first dissolved in the solvent–buffer mixture before the addition of plant material. Extraction time and stirring conditions were also set according to the BBD. All extractions were carried out in a thermoshaker (Thermomixer®, Eppendorf, Hamburg, Germany) at 50 °C. Following extraction, the samples were centrifuged at 10,000 rpm for 10 min at 4 °C. The resulting supernatants were collected and stored at − 18 °C until further analysis. The optimum extract from BBD was freeze-dried (Freeze dryer ALPHA 1–4, Braun Biotech International, Germany) and the resulting dry powder was reconstituted with the buffer used in EAE at a final concentration of 100 mg/mL before bioactivity assessment. All extraction experiments were carried out in triplicate.

Table 1 Independent variables and their levels employed in the Box–Behnken Design (BBD)

Coded symbols	Independent variables	Levels		
		− 1	0	1
X_1	Enzyme loading Cellic® Ctec3 (% v/v)	0.1	0.2	0.3
X_2	Enzyme loading Pectinex® Ultra Color (% v/v)	0.1	0.2	0.3
X_3	Enzyme loading Viscoferm® (% v/v)	0.2	0.4	0.6
X_4	Enzyme loading Neutrase® (% v/v)	0.1	0.15	0.2
X_5	Agitation (rpm)	300	800	1300
X_6	Extraction time (min)	60	90	120

Conventional extraction

For comparative purposes, conventional solvent extraction was performed following the procedure previously reported [17]. The milled material (6% w/v) was mixed with an ethanol–water solution (EtOH:H_2O 70:30 v/v), and extraction was performed under the optimal conditions determined by the BBD, allowing direct comparison with EAE. The extraction was carried out in a thermoshaker (Thermomixer®, Eppendorf, Hamburg, Germany) at 50 °C. After extraction, the samples were centrifuged at 10,000 rpm for 10 min at 4 °C. The collected supernatants were collected and stored at − 18 °C until further analysis. All extraction experiments were carried out in triplicate.

Biological activities

Antioxidant activity The antioxidant activity was evaluated by the DPPH radical scavenging assay, as previously described [16]. Briefly, different concentrations of the extract were mixed with a DPPH solution (2.5% w/v in methanol) and incubated in the dark at room temperature for 30 min. Absorbance was read at 515 nm, and the DPPH radical scavenging activity of the samples was quantified by the IC_{50} value expressed as µL of extract per mL of sample ($\mu L_{extract}/mL$) calculated from the linear regression of percentage inhibition of DPPH radicals vs. extract concentrations. All measurements were performed in triplicate.

Antibacterial activity The antibacterial activity of the extracts was tested against the gram-negative bacteria *Escherichia coli* (*E. coli*) DSM 6897 using the broth microdilution method as previously reported [16]. Optical density was recorded at 600 nm after 24 h of incubation using a 96-well microplate reader (SpectraMax ABS Plus, Molecular Devices, USA). Antibacterial activity was expressed as % inhibition of *E. coli* growth. All measurements were performed in triplicate.

Antidiabetic activity (α-amylase inhibition) Inhibition of α-amylase activity was performed using the iodine/potassium iodide (IKI) method, following a previously published protocol [16]. Briefly, the sample was mixed with α-amylase solution (0.5 U/mL) in a 96-well microplate and pre-incubated at 37 °C for 10 min. The

Table 2 The Box–Behnken Design and corresponding response values

A/A	X1	X2	X3	X4	X5	X6	TPC (mg GAE/g DW)	TFC (mg CAE/g DW)	Antioxidant activity (IC50, μL extract/mL)
1	+1(0.3)	0(0.2)	0(0.4)	−1(0.1)	−1(300)	0(90)	$100.4 \pm 3.14^{a***\beta*\mathbf{B}'***}$	$45.54 \pm 3.6^{a***\beta*\mathbf{B}'***}$	$0.91 \pm 0.00^{B\alpha'a*\mathbf{B}'***}$
2	+1(0.3)	0(0.2)	0(0.4)	+1(0.2)	−1(300)	0(90)	$106.39 \pm 4.28^{a***\alpha\beta\mathbf{B}'***}$	$33.68 \pm 1.46^{a***\beta\mathbf{B}'***}$	$0.88 \pm 0.17^{B\alpha'a*\mathbf{B}'***}$
3	0(0.2)	−1(0.1)	−1(0.2)	0(0.15)	−1(300)	0(90)	$106.51 \pm 2.23^{b***\alpha*\mathbf{B}'***}$	$36.49 \pm 2.12^{b***\alpha*\mathbf{B}'***}$	$0.79 \pm 0.09^{A\alpha'b*\mathbf{B}'***}$
4	0(0.2)	+1(0.3)	−1(0.2)	0(0.15)	−1(300)	0(90)	$103.67 \pm 1.24^{ab\alpha*\mathbf{B}'***}$	$33.88 \pm 0.31^{b\alpha*\mathbf{B}'***}$	$0.98 \pm 0.13^{A\alpha'ab\mathbf{B}'***}$
5	0(0.2)	−1(0.1)	1(0.6)	0(0.15)	−1(300)	0(90)	$91.39 \pm 2.87^{b***\alpha*\mathbf{B}'***}$	$34.72 \pm 1.22^{b***\alpha*\mathbf{B}'***}$	$0.99 \pm 0.^{1A\alpha'b*\mathbf{B}'***}$
6	0(0.2)	+1(0.3)	1(0.6)	0(0.15)	−1(300)	0(90)	$94.47 \pm 2.78^{ab\alpha*\mathbf{B}'***}$	$43.40 \pm 3.38^{b\alpha*\mathbf{B}'***}$	$0.97 \pm 0.^{19A\alpha'ab\mathbf{B}'***}$
7	0(0.2)	−1(0.1)	0(0.4)	0(0.15)	−1(300)	−1(60)	$98.57 \pm 2.93^{b***\alpha*\mathbf{B}'***}$	$40.67 \pm 1.48^{b***\alpha*\mathbf{B}'***}$	$0.87 \pm 0.^{00A\alpha'\beta'b*\mathbf{B}'***}$
8	0(0.2)	+1(0.3)	0(0.4)	0(0.15)	−1(300)	−1(60)	$103.15 \pm 1.25^{ab\alpha*\mathbf{B}'***}$	$31.6 \pm 1.92^{b\alpha*\mathbf{B}'***}$	$0.78 \pm 0.^{01A\alpha'\beta'ab\mathbf{B}'***}$
9	0(0.2)	−1(0.1)	0(0.4)	0(0.15)	−1(300)	+1(120)	$101.57 \pm 1.53^{b***\alpha*\mathbf{B}'***}$	$32.73 \pm 1.03^{b***\alpha*\mathbf{B}'***}$	$0.71 \pm 0.02^{A\beta'b*\mathbf{B}'***}$
10	0(0.2)	+1(0.3)	0(0.4)	0(0.15)	−1(300)	+1(120)	$116.28 \pm 0.33^{ab\alpha*\mathbf{B}'***}$	$55.84 \pm 0.31^{b\alpha*\mathbf{B}'***}$	$0.62 \pm 0.03^{A\beta'ab\mathbf{B}'***}$
11	−1(0.1)	0(0.2)	0(0.4)	−1(0.1)	−1(300)	0(90)	$105.95 \pm 2.37^{a***\beta*\mathbf{B}'***}$	$33.22 \pm 1.65^{a***\beta*\mathbf{B}'***}$	$1.01 \pm 0.05^{AB\alpha'a*\mathbf{B}'***}$
12	−1(0.1)	0(0.2)	0(0.4)	+1(0.2)	−1(300)	0(90)	$95.51 \pm 2.72^{a***\alpha\beta\mathbf{B}'***}$	$31.44 \pm 1.53^{a***\beta\mathbf{B}'***}$	$0.88 \pm 0.03^{AB\alpha'a*\mathbf{B}'***}$
13	+1(0.3)	−1(0.1)	0(0.4)	−1(0.1)	0(800)	0(90)	$117.09 \pm 1.96^{b***\beta*\mathbf{A}'***}$	$41.16 \pm 2.34^{b***\beta*\mathbf{A}'***}$	$0.66 \pm 0.34^{B\alpha'b*\mathbf{A}'***}$
14	+1(0.3)	+1(0.3)	0(0.4)	−1(0.1)	0(800)	0(90)	$115.45 \pm 2.25^{ab\beta*\mathbf{A}'***}$	$41.89 \pm 2.51^{b\beta*\mathbf{A}'***}$	$0.5 \pm 0.01^{B\alpha'ab\mathbf{A}'***}$
15	+1(0.3)	−1(0.1)	0(0.4)	+1(0.2)	0(800)	0(90)	$116.88 \pm 6.26^{b***\alpha\beta\mathbf{A}'***}$	$42.61 \pm 1.92^{b***\beta\mathbf{A}'***}$	$0.43 \pm 0.02^{B\alpha'b*\mathbf{A}'***}$
16	+1(0.3)	+1(0.3)	0(0.4)	+1(0.2)	0(800)	0(90)	$113.59 \pm 1.36^{ab\alpha\beta\mathbf{A}'***}$	$46.44 \pm 2.79^{b\beta\mathbf{A}'***}$	$0.78 \pm 0.01^{B\alpha'ab\mathbf{A}'***}$
17	+1(0.3)	0(0.2)	−1(0.2)	0(0.15)	0(800)	−1(60)	$119.77 \pm 3.01^{a***\alpha*\mathbf{A}'***}$	$50.70 \pm 2.66^{a***\alpha*\mathbf{A}'***}$	$0.66 \pm 0.03^{B\alpha'\beta'a*\mathbf{A}'***}$
18	+1(0.3)	0(0.2)	1(0.6)	0(0.15)	0(800)	−1(60)	$126.23 \pm 1.17^{a***\alpha*\mathbf{A}'***}$	$53.16 \pm 3.21^{a***\alpha*\mathbf{A}'***}$	$0.68 \pm 0.07^{B\alpha'\beta'a*\mathbf{A}'***}$
19	+1(0.3)	0(0.2)	−1(0.2)	0(0.15)	0(800)	+1(120)	$121.73 \pm 3.27^{a***\alpha*\mathbf{A}'***}$	$52.29 \pm 3.14^{a***\alpha*\mathbf{A}'***}$	$0.56 \pm 0.09^{B\beta'a*\mathbf{A}'***}$
20	+1(0.3)	0(0.2)	1(0.6)	0(0.15)	0(800)	+1(120)	$119.25 \pm 2.66^{a***\alpha*\mathbf{A}'***}$	$49.15 \pm 2.94^{a***\alpha*\mathbf{A}'***}$	$0.79 \pm 0.04^{B\beta'a*\mathbf{A}'***}$
21	0(0.2)	0(0.2)	−1(0.2)	−1(0.1)	0(800)	−1(60)	$111.01 \pm 3.86^{a***\beta*\mathbf{A}'***}$	$48.27 \pm 2.67^{a***\beta*\mathbf{A}'***}$	$0.79 \pm 0.01^{A\alpha'\beta'a*\mathbf{A}'***}$
22	0(0.2)	0(0.2)	1(0.6)	−1(0.1)	0(800)	−1(60)	$114.44 \pm 3.95^{a***\beta*\mathbf{A}'***}$	$41.39 \pm 3.83^{a***\beta*\mathbf{A}'***}$	$0.76 \pm 0.03^{A\alpha'\beta'a*\mathbf{A}'***}$
23	0(0.2)	0(0.2)	−1(0.2)	+1(0.2)	0(800)	−1(60)	$119.06 \pm 2.47^{a***\alpha\beta\mathbf{A}'***}$	$44.94 \pm 2.85^{a***\beta\mathbf{A}'***}$	$0.82 \pm 0.02^{A\alpha'\beta'a*\mathbf{A}'***}$
24	0(0.2)	0(0.2)	1(0.6)	+1(0.2)	0(800)	−1(60)	$113.14 \pm 1.98^{a***\alpha\beta\mathbf{A}'***}$	$46.2 \pm 2.01^{a***\beta\mathbf{A}'***}$	$0.78 \pm 0.00^{A\alpha'\beta'a*\mathbf{A}'***}$
25	0(0.2)	0(0.2)	−1(0.2)	−1(0.1)	0(800)	+1(120)	$119.01 \pm 6.03^{a***\beta*\mathbf{A}'***}$	$53.23 \pm 3.19^{a***\beta*\mathbf{A}'***}$	$0.76 \pm 0.02^{A\beta'a*\mathbf{A}'***}$
26	0(0.2)	0(0.2)	1(0.6)	−1(0.1)	0(800)	+1(120)	$121.71 \pm 3.69^{a***\beta*\mathbf{A}'***}$	$46.41 \pm 2.15^{a***\beta*\mathbf{A}'***}$	$0.75 \pm 0.04^{A\beta'a*\mathbf{A}'***}$
27	0(0.2)	0(0.2)	−1(0.2)	+1(0.2)	0(800)	+1(120)	$118.66 \pm 2.64^{a***\alpha\beta\mathbf{A}'***}$	$44.47 \pm 2.47^{a***\beta\mathbf{A}'***}$	$0.77 \pm 0.01^{A\beta'a*\mathbf{A}'***}$
28	0(0.2)	0(0.2)	1(0.6)	+1(0.2)	0(800)	+1(120)	$122.01 \pm 3.77^{a***\alpha\beta\mathbf{A}'***}$	$45.46 \pm 2.73^{a***\beta\mathbf{A}'***}$	$0.69 \pm 0.02^{A\beta'a*\mathbf{A}'***}$
29	0(0.2)	0(0.2)	0(0.4)	0(0.15)	0(800)	0(90)	$126.07 \pm 2.47^{a***\alpha*\mathbf{A}'***}$	$59.26 \pm 3.55^{a***\alpha*\mathbf{A}'***}$	$0.73 \pm 0.13^{A\alpha'a*\mathbf{A}'***}$
30	0(0.2)	0(0.2)	0(0.4)	0(0.15)	0(800)	0(90)	$132.77 \pm 1.20^{a***\alpha*\mathbf{A}'***}$	$54.9 \pm 3.31^{a***\alpha*\mathbf{A}'***}$	$0.67 \pm 0.03^{A\alpha'a*\mathbf{A}'***}$
31	0(0.2)	0(0.2)	0(0.4)	0(0.15)	0(800)	0(90)	$124.8 \pm 1.18^{a***\alpha*\mathbf{A}'***}$	$56.73 \pm 3.42^{a***\alpha*\mathbf{A}'***}$	$0.84 \pm 0.00^{A\alpha'a*\mathbf{A}'***}$
32	0(0.2)	0(0.2)	0(0.4)	0(0.15)	0(800)	0(90)	$125.77 \pm 1.89^{a***\alpha*\mathbf{A}'***}$	$55.61 \pm 3.34^{a***\alpha*\mathbf{A}'***}$	$0.83 \pm 0.12^{A\alpha'a*\mathbf{A}'***}$
33	0(0.2)	0(0.2)	0(0.4)	0(0.15)	0(800)	0(90)	$125.95 \pm 5.13^{a***\alpha*\mathbf{A}'***}$	$56.06 \pm 3.37^{a***\alpha*\mathbf{A}'***}$	$0.78 \pm 0.07^{A\alpha'a*\mathbf{A}'***}$
34	0(0.2)	0(0.2)	0(0.4)	0(0.15)	0(800)	0(90)	$122.02 \pm 2.60^{a***\alpha*\mathbf{A}'***}$	$54.93 \pm 3.30^{a***\alpha*\mathbf{A}'***}$	$0.71 \pm 0.02^{A\alpha'a*\mathbf{A}'***}$
35	−1(0.1)	−1(0.1)	0(0.4)	−1(0.1)	0(800)	0(90)	$113.47 \pm 2.39^{b***\beta*\mathbf{A}'***}$	$44.55 \pm 2.48^{b***\beta*\mathbf{A}'***}$	$0.55 \pm 0.03^{AB\alpha'b*\mathbf{A}'***}$
36	−1(0.1)	+1(0.3)	0(0.4)	−1(0.1)	0(800)	0(90)	$116.79 \pm 2.8^{ab\beta*\mathbf{A}'***}$	$35.31 \pm 2.13^{b\beta*\mathbf{A}'***}$	$0.68 \pm 0.17^{AB\alpha'ab\mathbf{A}'***}$
37	−1(0.1)	−1(0.1)	0(0.4)	+1(0.2)	0(800)	0(90)	$119.26 \pm 3.06^{b***\alpha\beta\mathbf{A}'***}$	$38.41 \pm 2.18^{b***\beta\mathbf{A}'***}$	$0.52 \pm 0.02^{AB\alpha'b*\mathbf{A}'***}$
38	−1(0.1)	+1(0.3)	0(0.4)	+1(0.2)	0(800)	0(90)	$120.41 \pm 2.89^{ab\alpha\beta\mathbf{A}'***}$	$51.08 \pm 3.07^{b\beta\mathbf{A}'***}$	$0.72 \pm 0.01^{AB\alpha'ab\mathbf{A}'***}$
39	−1(0.1)	0(0.2)	−1(0.2)	0(0.15)	0(800)	−1(60)	$123.49 \pm 6.31^{a***\alpha*\mathbf{A}'***}$	$49.89 \pm 2.72^{a***\alpha*\mathbf{A}'***}$	$0.7 \pm 0.14^{AB\alpha'\beta'a*\mathbf{A}'***}$
40	−1(0.1)	0(0.2)	1(0.6)	0(0.15)	0(800)	−1(60)	$119.61 \pm 2.22^{a***\alpha*\mathbf{A}'***}$	$52.55 \pm 3.17^{a***\alpha*\mathbf{A}'***}$	$0.72 \pm 0.02^{AB\alpha'\beta'a*\mathbf{A}'***}$
41	−1(0.1)	0(0.2)	−1(0.2)	0(0.15)	0(800)	+1(120)	$124.39 \pm 3.67^{a***\alpha*\mathbf{A}'***}$	$52.89 \pm 2.88^{a***\alpha*\mathbf{A}'***}$	$0.68 \pm 0.11^{AB\beta'a*\mathbf{A}'***}$
42	−1(0.1)	0(0.2)	1(0.6)	0(0.15)	0(800)	+1(120)	$121.06 \pm 2.49^{a***\alpha*\mathbf{A}'***}$	$52.51 \pm 3.15^{a***\alpha*\mathbf{A}'***}$	$0.88 \pm 0.01^{AB\beta'a*\mathbf{A}'***}$
43	+1(0.3)	0(0.2)	0(0.4)	−1(0.1)	+1(1300)	0(90)	$119.30 \pm 4.13^{a***\beta*\Gamma'***}$	$45.07 \pm 3.01^{a***\beta*\mathbf{A}'***}$	$0.83 \pm 0.01^{B\alpha'a*\mathbf{B}'}$
44	+1(0.3)	0(0.2)	0(0.4)	+1(0.2)	+1(1300)	0(90)	$120.10 \pm 3.38^{a***\alpha\beta\Gamma'***}$	$49.62 \pm 3.79^{a***\beta\mathbf{A}'***}$	$0.74 \pm 0.04^{B\alpha'a*\mathbf{B}'}$
45	0(0.2)	−1(0.1)	−1(0.2)	0(0.15)	+1(1300)	0(90)	$128.41 \pm 6.31^{b***\alpha*\Gamma'***}$	$47.51 \pm 6.24^{b***\alpha*\mathbf{A}'***}$	$0.92 \pm 0.00^{A\alpha'b*\mathbf{B}'}$
46	0(0.2)	+1(0.3)	−1(0.2)	0(0.15)	+1(1300)	0(90)	$121.04 \pm 2.34^{ab\alpha*\Gamma'***}$	$45.79 \pm 3.96^{b\alpha*\mathbf{A}'***}$	$1.14 \pm 0.09^{A\alpha'ab\mathbf{B}'}$
47	0(0.2)	−1(0.1)	1(0.6)	0(0.15)	+1(1300)	0(90)	$122.05 \pm 2.82^{b***\alpha*\Gamma'***}$	$43.03 \pm 0.67^{b***\alpha*\mathbf{A}'***}$	$0.83 \pm 0.04^{A\alpha'b*\mathbf{B}'}$
48	0(0.2)	+1(0.3)	1(0.6)	0(0.15)	+1(1300)	0(90)	$123.06 \pm 2.48^{ab\alpha*\Gamma'***}$	$42.92 \pm 2.24^{b\alpha*\mathbf{A}'***}$	$0.96 \pm 0.03^{A\alpha'ab\mathbf{B}'}$

Table 2 (continued)

A/A	X1	X2	X3	X4	X5	X6	TPC (mg GAE/g DW)	TFC (mg CAE/g DW)	Antioxidant activity (IC50, µL extract/mL)
49	0(0.2)	−1(0.1)	0(0.4)	0(0.15)	+1(1300)	−1(60)	$121.28 \pm 3.88^{b***\alpha*\Gamma'***}$	$52.23 \pm 4.88^{b***\alpha*A'***}$	$0.7 \pm 0.04^{A\alpha'\beta'b*B'}$
50	0(0.2)	+1(0.3)	0(0.4)	0(0.15)	+1(1300)	−1(60)	$125.97 \pm 3.6^{ab\alpha*\Gamma'***}$	$51.75 \pm 0.92^{b\alpha*A'***}$	$0.75 \pm 0.04^{A\alpha'\beta'abB'}$
51	0(0.2)	−1(0.1)	0(0.4)	0(0.15)	+1(1300)	+1(120)	$117.33 \pm 3.5^{b***\alpha*\Gamma'***}$	$41.91 \pm 4.38^{b***\alpha*A'***}$	$0.73 \pm 0.02^{A\beta'b*B'}$
52	0(0.2)	+1(0.3)	0(0.4)	0(0.15)	+1(1300)	+1(120)	$133.36 \pm 2.65^{ab\alpha*\Gamma'***}$	$44.19 \pm 3.42^{b\alpha*A'***}$	$0.72 \pm 0.03^{A\beta'abB'}$
53	−1(0.1)	0(0.2)	0(0.4)	−1(0.1)	+1(1300)	0(90)	$122.98 \pm 2.84^{a***\beta*\Gamma'***}$	$46.39 \pm 1.53^{a***\beta*A'***}$	$0.89 \pm 0.01^{AB\alpha'a*B'}$
54	−1(0.1)	0(0.2)	0(0.4)	+1(0.2)	+1(1300)	0(90)	$133.87 \pm 0.99^{a***\beta*\Gamma'***}$	$49.86 \pm 3.17^{a***\beta*A'***}$	$0.86 \pm 0.05^{AB\alpha'a*B'}$

The results are expressed as mean values ± SD. Letters per variable: X1 (A–C). X2 (a–c), X3 (A–Γ), X4 (α–γ), X5 (A′–Γ′), X6 (α′–γ′). Same letters indicate no statistically significant difference, while different letters indicate a statistically significant difference. Asterisks denote the level of significance (*$p < 0.05$, **$p < 0.01$, ***$p < 0.001$)

enzymatic reaction was initiated by adding starch solution (0.025% w/v), followed by a second 10-min incubation at 37 °C. The reaction was terminated by adding 1 M HCl, after which iodine–potassium iodide reagent was added. Absorbance was read at 630 nm using a 96-well microplate reader (SpectraMax ABS Plus, Molecular Devices, USA). Acarbose was used as the positive control (complete inhibition of α-amylase activity). Antidiabetic activity was determined by the IC_{50} value, calculated by the linear plot of extract concentrations (20–100 mg/mL) versus percentage inhibition of α-amylase, and the results were finally expressed as mg of extract per mL of sample. All measurements were performed in triplicate.

Anti-aging activity (tyrosinase inhibition) Inhibition of tyrosinase was measured using a modified dopachrome assay as previously published with L-DOPA as substrate [16]. Samples were incubated with tyrosinase (200 U/mL), phosphate buffer (50 mM), and L-DOPA (10 mM). The reaction mixtures were incubated at 25 °C for 10 min. Absorbance was read at 492 nm using a 96-well microplate reader (SpectraMax ABS Plus, Molecular Devices, USA). Kojic acid served as the positive control (complete inhibition of tyrosinase activity). Anti-aging activity was expressed as IC_{50} values, calculated from linear regression analysis of extract concentration (10–60 mg/mL) versus percentage tyrosinase inhibition and reported as mg extract per mL of sample. All measurements were performed in triplicate.

Total phenolic content Total phenolic content was determined according to the Folin–Ciocalteu colorimetric assay, as previously described [16]. The extract was mixed with Folin–Ciocalteu reagent, aqueous sodium carbonate solution (22% w/v), and distilled water. The reaction mixture was incubated at ambient temperature for 1 h. Absorbance was measured at 755 nm, and results were expressed as mg of gallic acid equivalents (GAE) per g of dry weight (DW) (mg GAE/g DW) using a gallic acid calibration curve ($C_{GAE} = 0.9377ABS_{755\ nm} + 0.0515$, $R^2 = 0.999$). All measurements were performed in triplicate.

Total flavonoid content Total flavonoid content was quantified based on the aluminum chloride colorimetric method, following the procedure reported in our previous study [16]. Briefly, the extract was mixed with sodium nitrite ($NaNO_2$), aluminum chloride ($AlCl_3$), sodium hydroxide (NaOH), and distilled water. After incubation at ambient temperature for 15 min, absorbance was read at 510 nm. The results were expressed as mg catechin equivalents (CAE) per g of dry weight (DW) (mg CAE/g DW) using a catechin calibration curve ($C_{CAE} = 0.8726ABS_{510\ nm} - 0.021$, $R^2 = 0.998$). All measurements were performed in triplicate.

Statistical analysis

Statistical evaluation of the experimental data was performed using Design-Expert 12.0 software (Stat-Ease Inc., Minneapolis, MN, USA—Trial Version). Before analysis, data normality and variance homogeneity were verified using the Shapiro–Wilk Test and Levene's Test, respectively. The significance of factor effects and model terms was assessed by analysis of variance (ANOVA) followed by Tukey's HSD test for multiple comparisons. The results were expressed as mean values ± standard deviation (SD) of three independent measurements ($n = 3$), and statistical significance was assumed at $p < 0.05$. Model performance was evaluated through determination coefficients (R^2, adjusted R^2, and predicted R^2), while Pareto charts of standardized effects were constructed using R software.

Results and discussion

The Box–Behnken experimental design (BBD) of six factors with three levels was applied to investigate the combined effect of six independent variables, namely the enzyme loading of four commercial enzyme preparations, Cellic® CTec3 HS, Pectinex® Ultra Color, Viscoferm®, and Neutrase®, agitation, and extraction time. The dependent variables of the model examined are the total phenolic content (TPC), the total flavonoid content (TFC), and the antioxidant activity. ANOVA was performed on the experimental data, followed by a post-hoc test, Tukey's HSD, to determine statistically significant differences between the means. Regression analysis was also conducted, and the resulting models were used to predict responses beyond the initially defined parameter limits. The data obtained from the BBD are presented in Table 2.

Antioxidant activity

Oxidative damage is associated with the onset of chronic diseases, including cardiovascular and neurodegenerative diseases, as well as cancer. Antioxidants mitigate oxidative damage by neutralizing the free radicals. Specifically, antioxidants of plant origin are distinguished by their high radical-scavenging capacity.

Experimentally, antioxidant activity (expressed in IC_{50} index) ranged from 0.43 ± 0.02 to 1.14 ± 0.09 μL extract/mL, demonstrating substantial variation among conditions (Table 2). The highest antioxidant activity occurred at high Cellic® CTec3 HS and Neutrase® loads, low Pectinex® Ultra Color, and medium Viscoferm® concentrations. IC_{50} values were minimized at medium agitation, while extraction time had a negligible effect. A notable 20% increase in antioxidant activity was observed between experiments 44 and 45, where Pectinex® and Viscoferm® were applied at medium levels, while at the highest agitation speed.

Table 3 presents the (Analysis of Variance) ANOVA results for the unmodified and modified mathematical models. The data were fitted to a quadratic model in coded (Eq. 1) and in actual values (Eq. 2), and the model showed a high F-value (10.76, p-value < 0.0001), confirming significance, while a non-significant lack-of-fit F-value (1.17, p-value > 0.05) indicated a good fit. The R^2 (0.8231), adjusted R^2 (0.7465), and predicted R^2 (0.6250) values were consistent, whereas the adequate precision of 15.37 verified signal strength. The close alignment of predicted and actual values (Fig. 1a) further supported the reliability of the model. These findings were further supported by the Pareto chart (Fig. 2a), which confirmed the significance of the model terms. According to the model equation (Eq. 5), the enzyme loading of Viscoferm® (% v/v) and Neutrase® (% v/v), as well as the extraction time, acted competitively, reducing the IC_{50} index, thus increasing the antioxidant activity. When Pectinex® Ultra Color was combined with either Cellic® CTec3 HS or Neutrase®, the antioxidant activity decreased, whereas its combination with Viscoferm® enhanced it.

$$\begin{aligned} Antioxidant\ Activity\ (\mu L_{extract}/\ mL) &= 0,7673 - 0,0108X_1 + 0,0419X_2 + 0,0099X_3 + 0,0082X_4 \\ &+ 0,009X_5 - 0,0192X_6 + 0,0632X_1X_5 - 0,03X_2X_3 + 0,0716X_2X_4 + 0,0335X_2X_5 - 0,0581X_3X_5 \\ &- 0,0392X_1^2 - 0,1265X_2^2 + 0,093X_3^2 + 0,2155X_5^2 - 0,1045X_6^2 \end{aligned} \quad (1)$$

$$\begin{aligned} Antioxidant\ Activity\ (\mu L_{extract}/\ mL) &= 0.43 + 0.45C + 3.55P - 0.97V - 2.70N - 0.0015A \\ &+ 0.02t + 0.0013CA - 1.88PV + 14.32PN + 0.001PA - 0.001VA - 3.93C^2 - 12.65P^2 \\ &+ 2.32V^2 + 0.0000009A^2 - 0.00012t^2 \end{aligned} \quad (2)$$

The 3D surface plots showed the existence of inflection points, meaning that the model did not present either a minimum or a maximum. Specifically, in Fig. 3a–d, this behavior was confirmed by the coefficients of the variables, where their value tend to zero. In Fig. 3e, the synergistic effect of the Viscoferm® loading with the agitation, for medium values of both, minimized the IC_{50} index.

Bioactive compounds

Total phenolic content (TPC) data ranged between 91.39 ± 2.87 and 133.87 ± 0.99 mg GAE/g DW (Table 2), indicating that different experimental conditions notably influenced the extraction yield. The lowest values of TPC were observed under low agitation conditions (300 rpm),

Table 3 ANOVA results for the unmodified and modified quadratic models fitted to the antioxidant activity data of *Rosa canina* L. extracts

	Unmodified				Modified			
	Sum of squares	**Mean square**	***F*-value**	***p*-value**	**Sum of squares**	**Mean square**	***F*-value**	***p*-value**
Model	0.9679	0.0358	5.74	< 0.0001	0.93	0.0581	10.76	< 0.0001
X_1	0.0028	0.0028	0.4491	0.5087	0.003	0.0028	0.5187	0.4759
X_2	0.0422	0.0422	6.76	0.0152	0.042	0.0422	7.8	0.0082
X_3	0.0024	0.0024	0.3782	0.5439	0.002	0.0024	0.4368	0.5128
X_4	0.0016	0.0016	0.2561	0.6171	0.002	0.0016	0.2958	0.5898
X_5	0.002	0.002	0.3126	0.5809	0.002	0.002	0.361	0.5516
X_6	0.0089	0.0089	1.42	0.2442	0.009	0.0089	1.64	0.2083
X_1X_2	0.0023	0.0023	0.3634	0.5518	-	-	-	-
X_1X_3	0.00	0.00	0.0064	0.9368	-	-	-	-
X_1X_4	0.0053	0.0053	0.857	0.3631	-	-	-	-
X_1X_5	0.0319	0.0319	5.11	0.0324	0.032	0.0319	5.9	0.0201
X_1X_6	0.0023	0.0023	0.3688	0.5489	-	-	-	-
X_2X_3	0.0113	0.0113	1.81	0.1896	0.011	0.0113	2.1	0.1562
X_2X_4	0.041	0.041	6.57	0.0165	0.041	0.041	7.59	0.0091
X_2X_5	0.018	0.018	2.88	0.1017	0.018	0.018	3.32	0.0764
X_2X_6	0.0041	0.0041	0.6575	0.4248	-	-	-	-
X_3X_4	0.0007	0.0007	0.1143	0.7381	-	-	-	-
X_3X_5	0.027	0.027	4.32	0.0477	0.027	0.027	4.99	0.0316
X_3X_6	0.0081	0.0081	1.3	0.265	-	-	-	-
X_4X_5	0.0076	0.0076	1.22	0.2788	-	-	-	-
X_4X_6	0.001	0.001	0.1567	0.6954	-	-	-	-
X_5X_6	0.0047	0.0047	0.7592	0.3915	-	-	-	-
X_1^2	0.0187	0.0187	3,00	0.0953	0.017	0.0173	3.19	0.0822
X_2^2	0.1603	0.1603	25.67	< 0.0001	0.168	0.1681	31.1	< 0.0001
X_3^2	0.0922	0.0922	14.76	0.0007	0.091	0.0907	16.79	0.0002
X_4^2	0.0015	0.0015	0.2333	0.6331	-	-	-	-
X_5^2	0.4853	0.4853	77.74	< 0.0001	0.488	0.4877	90.23	< 0.0001
X_6^2	0.1087	0.1087	17.41	0.0003	0.115	0.1147	21.21	< 0.0001
Lack of fit	0.1388	0.0066	1.41	0.3778	0.177	0.0055	1.17	0.4761

ranging from 91.39 ± 2.87 to 106.51 ± 2.23 mg GAE/g DW, suggesting that stirring intensity and mass transfer phenomena positively contribute to the release of phenolics from the plant material. The maximum value of TPC occurred in experiment 54 (133.87 ± 0.99 mg GAE/g DW), combining high values of agitation (1300 rpm), high enzyme loading of Neutrase® (0.2% v/v), while maintaining moderate Pectinex® Ultra Color (0.2% v/v) and Viscoferm® (0.4% v/v) levels, and a low enzyme loading of Cellic® CTec3 HS (0.1% v/v).

The TPC data were fitted to the quadratic polynomial model, and coefficient significance was determined at a 95% confidence level. Terms with p-value > 0.05 that did not improve model fit were excluded, except for main factors to retain the model hierarchy. Table 4 presents the ANOVA results for the unmodified and modified mathematical models, while the proposed model description equations are given in coded (Eq. 3) and actual values (Eq. 4). ANOVA results confirmed the model's adequacy. The statistical analysis confirmed the significance of the developed model, evidenced by an F-value of 16.12 and a p-value below 0.0001, with a non-significant lack-of-fit ($F = 1.47$ and p-value = 0.3594).

The R^2 (0.8745), adjusted R^2 (0.8202), and predicted R^2 (0.7102) values agreed satisfactorily (difference between adjusted R^2 and predicted R^2 below 0.2), demonstrating satisfactory predictive performance [25]. The adequate precision value of 16.651 demonstrated a strong signal-to-noise ratio, confirming that the model can predict TPC responses within the experimental range. As shown

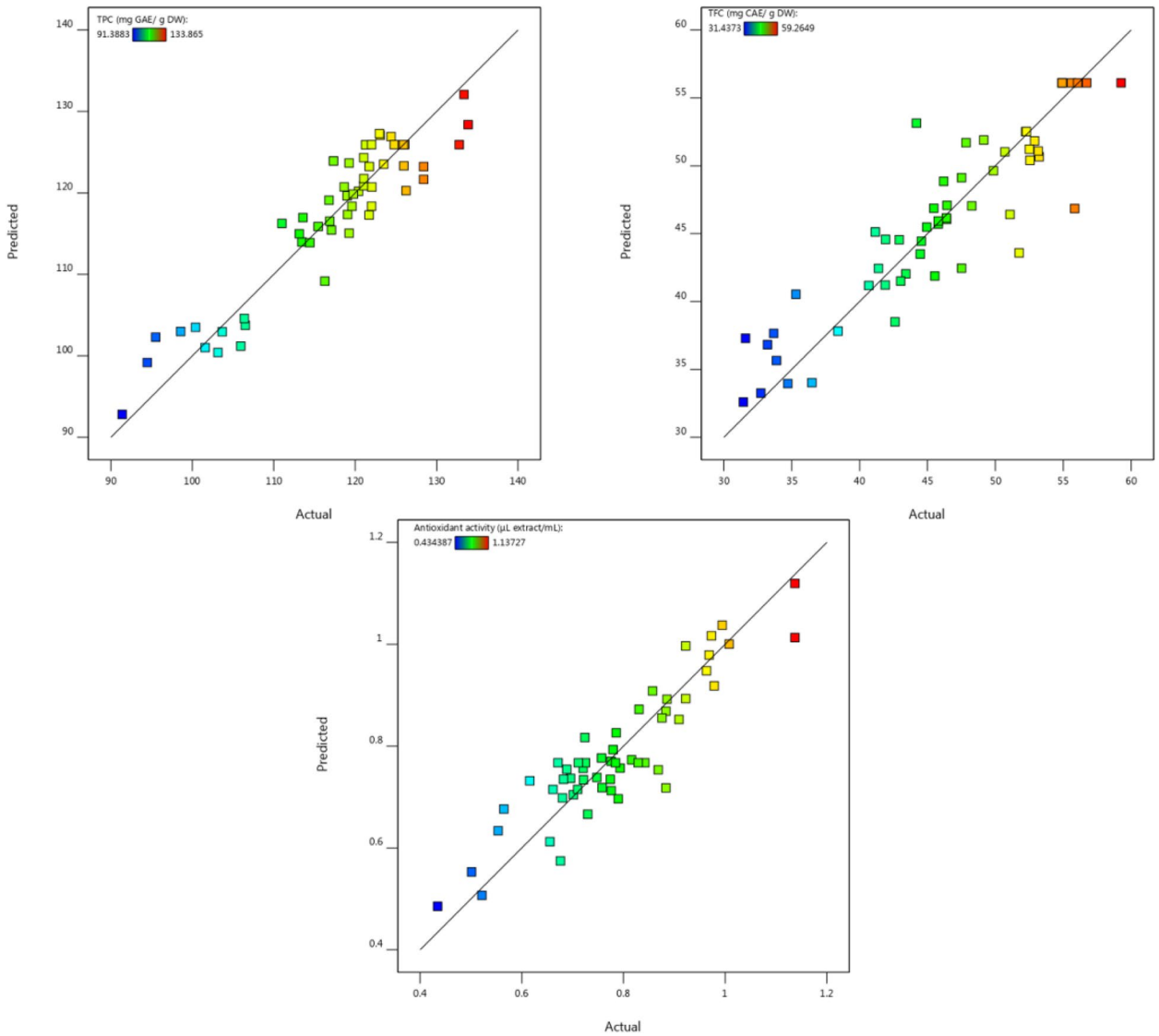


Fig. 1 Correlation between predicted and actual values for **a** antioxidant activity, **b** total phenolic content (TPC), and **c** total flavonoid content (TFC) of the extracts obtained from the Box–Behnken Design (BBD)

in Fig. 1b, predicted versus actual TPC values aligned closely along the diagonal, further validating model accuracy. The Pareto chart (Fig. 2b) illustrates that factors within the reference line (p-value = 0.05) contributed minimally to TPC prediction.

According to the regression coefficients (Eq. 3), extraction time had a slightly antagonistic effect, whereas the remaining variables exerted positive influences, with Neutrase® loading showing the strongest linear effect. The interactions between Viscoferm®–Pectinex® Ultra Color and Viscoferm®–Cellic® CTec3 HS were synergistic, enhancing phenolic release when these enzymes were used together at high concentrations. Conversely, the Cellic® CTec3 HS–Pectinex® Ultra Color combination exhibited a competitive interaction, reducing TPC yields.

$$\begin{aligned} TPC\ (mg\ GAE/\ g\ DW) &= 125.9 - 0.44X_1 + 1.39X_2 - 1.18X_3 + 0.55X_4 + 11.46X_5 \\ &+ 1.69X_6 - 1.17X_1X_2 + 1.40X_1X_3 - 1.59X_1X_5 + 1.79X_2X_3 + 2.68X_2X_6 + 2.50X_3X_6 \\ &- 4.39X_2^2 - 3.72X_3^2 - 4.89X_4^2 - 6.69X_5^2 \end{aligned} \quad (3)$$

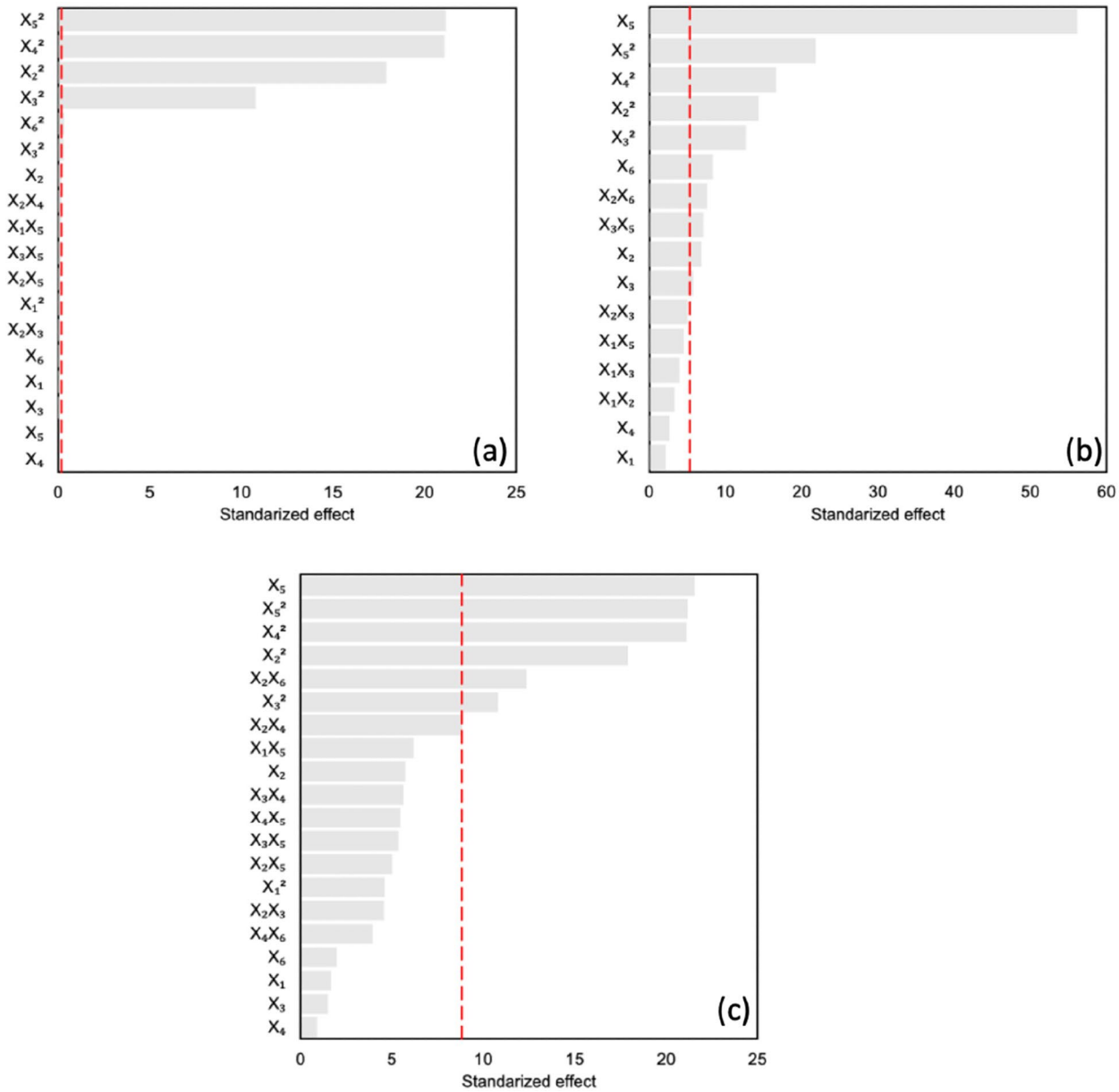


Fig. 2 Pareto chart of standardized effects for **a** antioxidant activity, **b** TPC, **c** TFC of the extracts from BBD. The dashed line represents the significance threshold at *p*-value = 0.05; effects with bars extending beyond this line are considered statistically significant ($p < 0.05$)

$$TPC\ (mg\ GAE/g\ DW) = 34.84 + 16.52C + 96.64P + 16.70V + 597.53N + 0.06A - 0.12t - 117.48CP + 70.01CV - 0.032CA + 89.38PV + 0.89Pt + 0.025VA - 438.66P^2 - 93.07V^2 - 1955.33N^2 - 0.00003A^2 \quad (4)$$

where C = enzyme load of Cellic® CTec3 HS; P = enzyme load of Pectinex® Ultra Color; V = enzyme load of Viscoferm®; N = enzyme load of Neutrase®; A = agitation, and t = extraction time.

The relationship between the studied factors and the TPC was evaluated through three-dimensional (3D) response surface plots (Fig. 4a–f), illustrating the combined effects of two variables while keeping the remaining four at their average levels. The 3D plots confirm the

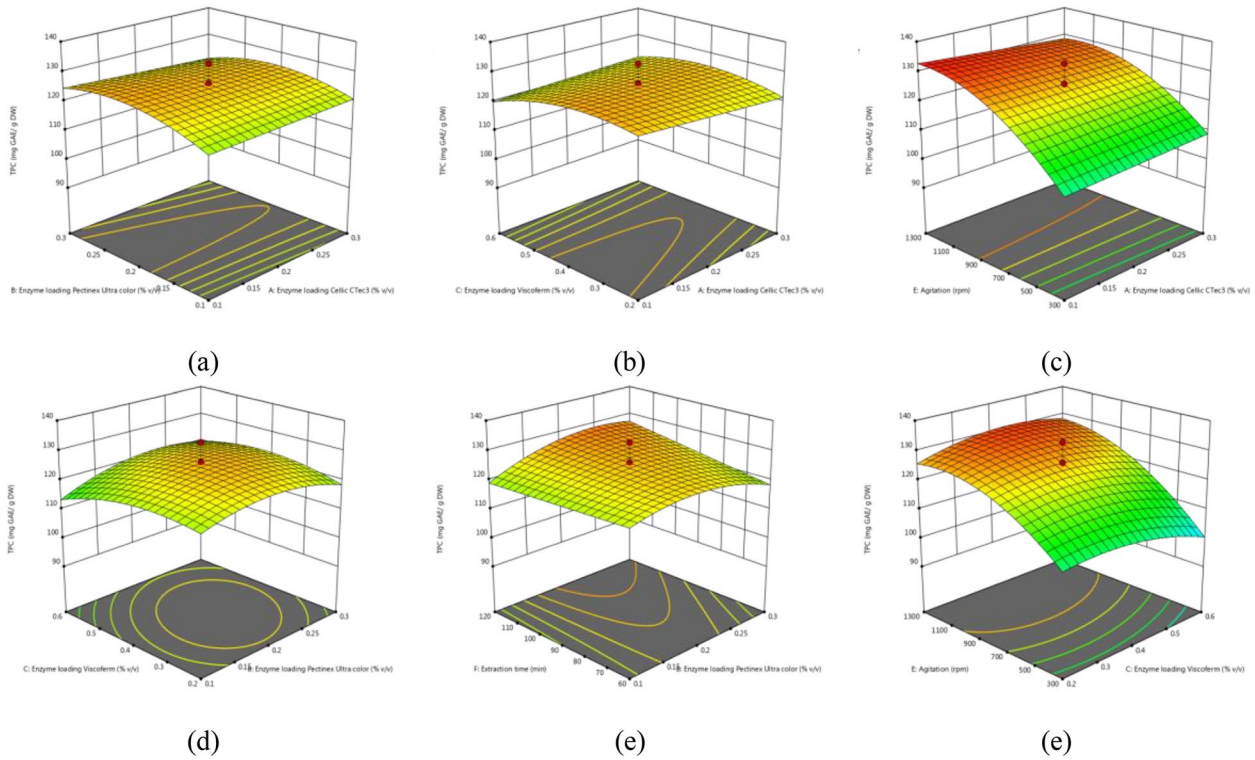


Fig. 3 Three-dimensional (3D) surface plot of the antioxidant activity response with the studied factors

previous analyses, showing that TPC is maximized at low Cellic® CTec3 HS loading (0.1% v/v) combined with medium Pectinex® Ultra Color (0.2% v/v) and Viscoferm® (0.3–0.4% v/v) concentrations (Figs. 4a and 3b). The cellulolytic enzyme had little effect on TPC at high agitation speeds (> 900 rpm), as indicated by the nearly linear response surface (Fig. 4c). The combination of Pectinex® Ultra Color and Viscoferm® showed a strong synergistic interaction, maximizing TPC at intermediate enzyme levels (0.3% and 0.2% v/v, respectively), as evidenced by the concentric contours in Fig. 4d. Similarly, high Pectinex® Ultra Color load combined with longer extraction time increases TPC, highlighting the synergistic effect of enzymatic cell wall degradation and prolonged solvent contact (Fig. 4e). Finally, high agitation speeds in the presence of medium hemicellulolytic levels produced a slight increase in TPC yield (Fig. 4f).

Total flavonoid content (TFC) values ranged from 31.4 ± 1.53 to 59.3 ± 3.55 mg CAE/g DW (Table 2). The highest TFC values occurred at medium stirring speed (800 rpm), while the lowest values were observed at low stirring speed (300 rpm), as in TPC. The maximum value of TFC of 59.3 ± 3.55 mg CAE/g DW corresponded to a central point. High enzyme loadings of Cellic® CTec3 HS, Pectinex® Ultra Color, and Neutrase® led to high TFC values, as shown in experiments 18, 19, and 38, respectively.

The response of TFC was described according to a quadratic model. Table 5 presents the ANOVA results for the unmodified and modified mathematical models. The final proposed model description equations are given in coded (Eq. 5) and actual values (Eq. 6). The lack-of-fit was statistically significant (p-value < 0.05), suggesting that the model does not perfectly predict the response, possibly due to the presence of outliers. The coefficient of determination ($R^2 = 0.8173$) indicated a satisfactory fit; however, the difference between adjusted and predicted R^2 (0.7065 and 0.4800, respectively) exceeded 0.2, implying limited predictive accuracy. Despite this, the adequate precision value (16.65) confirmed a strong signal-to-noise ratio. In such cases, where the discrepancy between adjusted and predicted R^2 exceeds the recommended threshold, the model may still be considered acceptable when supported by a statistically significant regression, a non-significant lack-of-fit, adequate precision values greater than 4, and good agreement between predicted and experimental results within the studied experimental domain [25]. Also, Fig. 1c depicts a satisfactory correlation between predicted and actual values of TFC. The Pareto chart (Fig. 2c) confirmed the statistical significance (p-value < 0.05) of those terms, which most strongly influenced TFC.

Table 4 ANOVA results for the unmodified and modified quadratic models fitted to the TPC data of *Rosa canina* L. extracts

	Unmodified				Modified			
	Sum of squares	**Mean square**	***F*-value**	***p*-value**	**Sum of squares**	**Mean square**	***F*-value**	***p*-value**
Model	4620.26	171.12	7.58	< 0.0001	4553.91	284.62	16.12	< 0.0001
X_1	4.64	4.64	0.21	0.654	4.64	4.64	0.26	0.6112
X_2	46.57	46.57	2.06	0.1629	46.57	46.57	2.64	0.1129
X_3	33.45	33.45	1.48	0.2345	33.45	33.45	1.89	0.177
X_4	7.16	7.16	0.32	0.5781	7.16	7.16	0.41	0.5282
X_5	3149.97	3149.97	139.49	< 0.0001	3149.97	3149.97	178.35	< 0.0001
X_6	68.81	68.81	3.05	0.0927	68.81	68.81	3.9	0.0559
X_1X_2	11.04	11.04	0.49	0.4906	11.04	11.04	0.63	0.4342
X_1X_3	15.68	15.68	0.69	0.4122	15.68	15.68	0.89	0.3521
X_1X_4	11.06	11.06	0.49	0.4903	-	-	-	-
X_1X_5	20.19	20.19	0.89	0.353	20.19	20.19	1.14	0.2919
X_1X_6	6.82	6.82	0.30	0.5874	-	-	-	-
X_2X_3	25.56	25.56	1.13	0.2971	25.56	25.56	1.45	0.2366
X_2X_4	1.82	1.82	0.08	0.7786	-	-	-	-
X_2X_5	1.67	1.67	0.07	0.788	-	-	-	-
X_2X_6	57.6	57.6	2.55	0.1223	57.6	57.6	3.26	0.0791
X_3X_4	9.46	9.46	0.42	0.5231	-	-	-	-
X_3X_5	49.88	49.88	2.21	0.1492	-	-	-	-
X_3X_6	0.00	0.00	0.00	0.993	49.88	49.88	2.82	0.1013
X_4X_5	7.95	7.95	0.35	0.558	-	-	-	-
X_4X_6	5.79	5.79	0.26	0.6168	-	-	-	-
X_5X_6	20.12	20.12	0.89	0.3539	-	-	-	-
X_1^2	0.89	0.89	0.04	0.8446	-	-	-	-
X_2^2	204.83	204.83	9.07	0.0057	205.25	205.25	11.62	0.0016
X_3^2	139.25	139.25	6.17	0.0198	161.26	161.26	9.13	0.0045
X_4^2	242.51	242.51	10.74	0.003	278.06	278.06	15.74	0.0003
X_5^2	470.38	470.38	20.83	0.0001	476.9	476.9	27.00	< 0.0001
X_6^2	1.02	1.02	0.045	0.8336	-	-	-	-
Lack of fit	524.21	24.96	1.98	0.2301	590.56	18.46	1.47	0.3594

$$\begin{aligned} TFC\ (mgCAE/g\ DW) &= 56,1 + 0,3388X_1 + 1,17X_2 - 0,3085X_3 - 0,1878X_4 + 4,4X_5 \\ &+ 0,4074X_6 - 2,19X_1X_5 + 1,61X_2X_3 + 3,13X_2X_4 - 1,26X_2X_5 + 4,37X_2X_6 + 1,99X_3X_4 \\ &- 1,89X_3X_5 + 1,92X_4X_5 - 1,4X_4X_6 - 1,42X_1^2 - 5,53X_2^2 - 3,22X_3^2 - 6,51X_4^2 - 6,53X_5^2 \end{aligned} \quad (5)$$

$$\begin{aligned} TFC\ (mg\ CAE/\ g\ DW) &= -27.07 + 95.21C - 4.11P + 32.01V + 595.31N + 0.06A - 0.14t \\ &- 0.04CA + 80.66PV + 625.12PN - 0.03PA + 1.46Pt + 199.34VN - 0.019VA + 0.077NA \\ &- 0.93Nt - 141.99C^2 - 552.85P^2 - 80.60V^2 - 2604.80N^2 - 0.000026A^2 \end{aligned} \quad (6)$$

According to the model equation (Eq. 5), Neutrase® exhibited the strongest synergistic effect, followed by Cellic® CTec3 HS and Viscoferm®, while Pectinex® Ultra Color showed a mild antagonistic influence. In contrast, the interactions of Pectinex® Ultra Color with Viscoferm® and Neutrase® displayed strong synergistic effects,

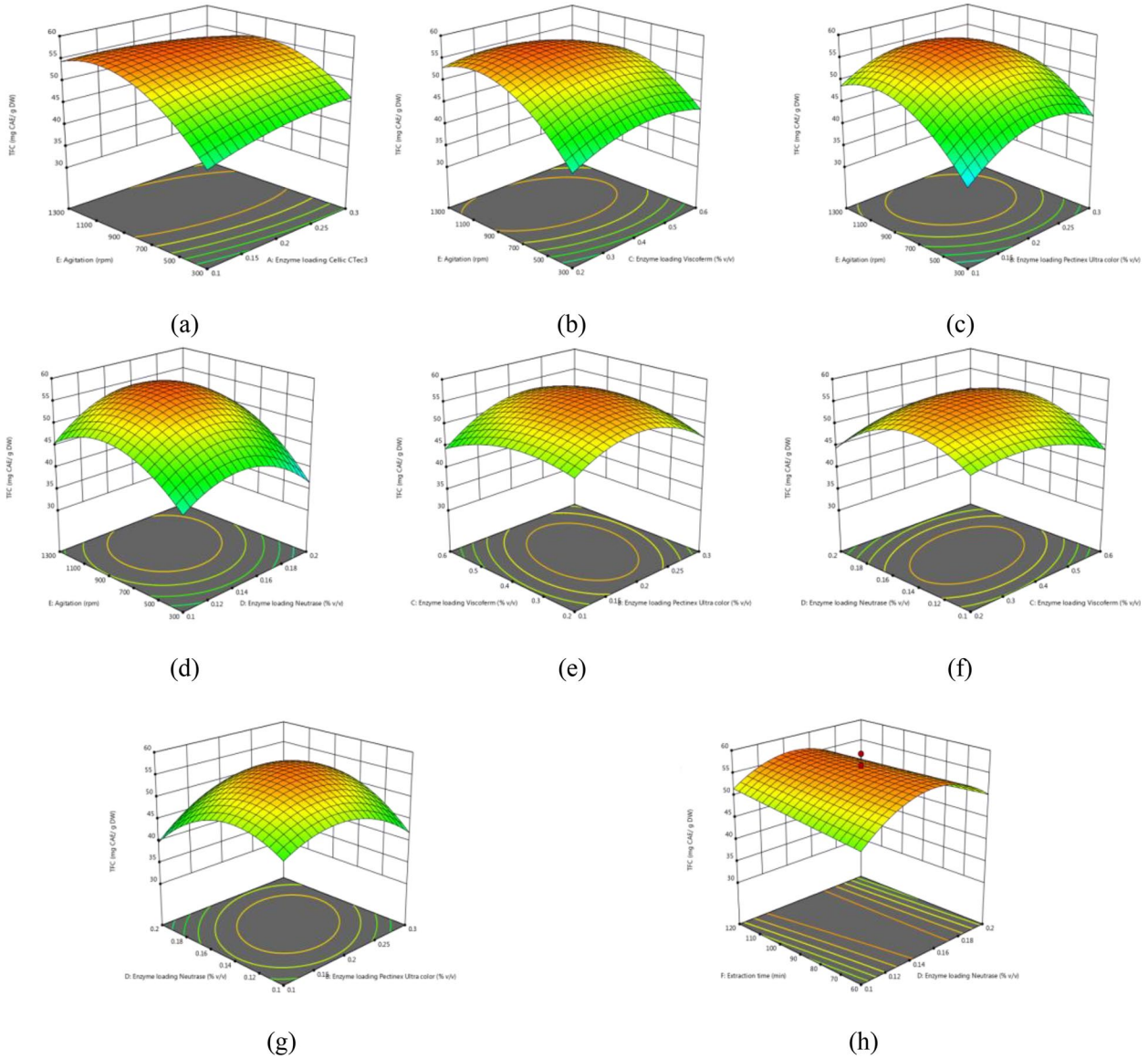


Fig. 4 Three-dimensional (3D) response surface plots of the total phenolic content (TPC) with the studied factors

suggesting that the combined use of these enzymes enhances cell wall degradation and the release of flavonoids, likely due to complementary enzymatic activity on the plant tissue structure. Increasing extraction time together with higher Pectinex® Ultra Color levels slightly enhanced TFC, suggesting that prolonged enzyme–substrate contact can improve efficiency.

The 3D surface plots (Fig. 5a–h) revealed that the TFC was mainly influenced by synergistic interactions among the enzyme loadings. Maximum TFC values were obtained at intermediate-to-low levels of cellulolytic and hemicellulolytic enzymes combined with relatively high agitation speeds (approximately 1100 rpm) (Fig. 5a, b). In contrast, the pectinolytic and proteolytic enzymes reached their optimal performance at slightly lower agitation rates, around 1000 rpm (Fig. 5c, d). Higher TFC values were consistently associated with medium loadings of the hemicellulolytic, pectinolytic, and proteolytic enzymes (Fig. 5e–g). Finally, Neutrase® exhibited a synergistic interaction with extraction time, with intermediate values of both factors yielding the highest TFC (Fig. 5h).

Optimization by desirability function

As discussed, each of the three responses was maximized under different optimal conditions. To identify a single

Table 5 ANOVA results for the unmodified and modified quadratic models fitted to the TFC data of *Rosa canina* L. extracts

	Unmodified				Modified			
	Sum of squares	**Mean square**	***F*-value**	***p*-value**	**Sum of squares**	**Mean square**	***F*-value**	***p*-value**
Model	2442.53	90.46	7.14	< 0.0001	2265.54	113.28	7.38	< 0.0001
X_1	2.76	2.76	0.22	0.6449	2.76	2.76	0.18	0.6746
X_2	32.84	32.84	2.59	0.1195	32.84	32.84	2.14	0.153
X_3	2.28	2.28	0.18	0.6747	2.28	2.28	0.15	0.7022
X_4	0.846	0.846	0.07	0.7982	0.85	0.85	0.06	0.8158
X_5	465.34	465.34	36.71	< 0.0001	465.34	465.34	30.32	< 0.0001
X_6	3.98	3.98	0.31	0.5799	3.98	3.98	0.26	0.6138
X_1X_2	0.16	0.16	0.01	0.9119	-	-	-	-
X_1X_3	0.06	0.06	0.01	0.9447	-	-	-	-
X_1X_4	22.3	22.3	1.76	0.1963	-	-	-	-
X_1X_5	38.34	38.34	3.02	0.0938	38.34	38.34	2.5	0.1235
X_1X_6	0.37	0.37	0.03	0.8661	-	-	-	-
X_2X_3	20.82	20.82	1.64	0.2113	20.82	20.82	1.36	0.2525
X_2X_4	78.15	78.15	6.17	0.0198	78.15	78.15	5.09	0.0308
X_2X_5	25.36	25.36	2.00	0.169	25.36	25.36	1.65	0.2076
X_2X_6	152.68	152.68	12.05	0.0018	152.68	152.68	9.95	0.0034
X_3X_4	31.79	31.79	2.51	0.1253	31.79	31.79	2.07	0.1595
X_3X_5	28.52	28.52	2.25	0.1457	28.52	28.52	1.86	0.1821
X_3X_6	7.43	7.43	0.59	0.4507	-	-	-	-
X_4X_5	29.64	29.64	2.34	0.1383	29.64	29.64	1.93	0.174
X_4X_6	15.67	15.67	1.24	0.2763	15.67	15.67	1.02	0.3196
X_5X_6	146.02	146.02	11.52	0.0022	-	-	-	-
X_1^2	21.81	21.81	1.72	0.2011	21.17	21.17	1.38	0.2486
X_2^2	318.5	318.5	25.13	< 0.0001	320.93	320.93	20.91	< 0.0001
X_3^2	102.18	102.18	8.06	0.0087	116.42	116.42	7.58	0.0095
X_4^2	441.03	441.03	34.8	< 0.0001	445.27	445.27	29.01	< 0.0001
X_5^2	443.22	443.22	34.97	< 0.0001	447.49	447.49	29.15	< 0.0001
X_6^2	0.6571	0.6571	0.05	0.8217	-	-	-	-
Lack of fit	316.19	15.06	5.64	0.0318	493.18	17.61	6.6	0.0221

set of factor levels that simultaneously maximizes all three dependent variables and minimizes the independent ones, the Derringer desirability function methodology was applied [26]. The optimal levels of the independent variables and the predicted values of the responses are presented in Table 6, where the desirability value (*D*) was 0.806, indicating a satisfactory level of optimization and a reasonable compromise between the targeted responses. Under the optimized extraction conditions, the predicted response values were 118.5 mg GAE/DW for total phenolic content (TPC), 50.0 mg CAE/g DW for total flavonoid content (TFC), and IC_{50} of 0.57 μL extract/mL for antioxidant activity. A confirmatory experiment was performed to confirm the overall accuracy of the models. The experimental results (Table 6) fell within lower and upper prediction limits, thereby confirming the validity of the model.

For comparative purposes, a commonly applied conventional extraction [17] was carried out using an ethanol:water mixture (70:30 v/v) for the optimum extraction time (60 min). The conventional extraction yielded a TPC of 55.01 ± 0.11 mg GAE/g DW, a TFC of 22.4 ± 1.30 mg CAE/g DW, and an antioxidant activity IC_{50} of 1.87 ± 0.03 μL extract/mL. When benchmarked against conventional ethanol–water extraction, the optimum extract of this study yielded about 50% higher both TPC and TFC, while about 60% higher antioxidant activity. Additionally, a control extraction conducted under identical conditions with buffer only (no enzyme) yielded 41.6 ± 1.8 mg GAE/g DW (TPC) and 20.9 ± 1.2 mg CAE/g DW (TFC). The present method balances both yield and efficiency, achieving high bioactive compounds extraction within a significantly short extraction time. This not only enhances the process's economic and environmental

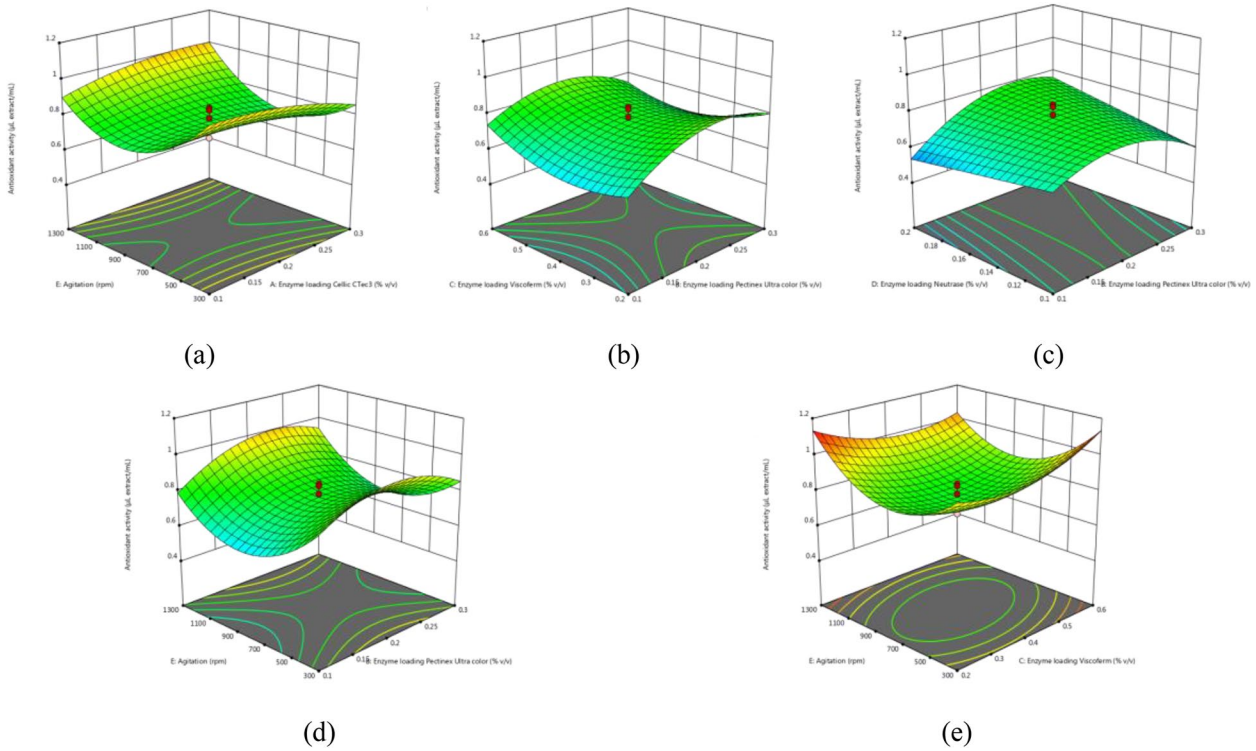


Fig. 5 Three-dimensional (3D) surface plot of the TFC response with the studied factors

sustainability but also minimizes the potential for oxidative degradation during extraction.

Several studies have reported a wide range of TPC and TFC values for *Rosa canina* L. depending on the extraction technique and conditions applied (Table 7). For instance, Ilbay et al. [11] optimized UAE and obtained a maximum TPC of 47.23 mg GAE/g using 40% (v/v) aqueous ethanol for 81.23 min, whereas ultrasound enzyme-assisted extraction (UAEE) using a pectinase–cellulase–hemicellulase mixture (0.6, 0.3, and 0.3 U/mL, respectively) achieved a TPC of 32.64 mg GAE/g [15]. In contrast, the UAE employing the green solvent γ-valerolactone (GVL) in a 70:30 (v/v) EtOH/GVL mixture yielded markedly lower values (up to 9.7 mg GAE/g DW), despite similar ultrasonic conditions [32]. Even higher recoveries have been reported using automatic solvent extraction, where extended extraction times (1 h 32 min) resulted in TPC values of 53.62 mg GAE/g DW and TFC values of 224.42 mg CE/g DW [31], although such discrepancies may also reflect differences in plant

Table 6 Optimized extraction conditions based on Derringer's desirability function, along with predicted and experimental (confirmation) values for TPC, TFC, and antioxidant activity

Independent variables		
Enzyme loading Cellic® CTec3 HS (% v/v)	0.1	
Enzyme loading Pectinex Ultra Color® (% v/v)	0.1	
Enzyme loading Viscoferm® (% v/v)	0.21	
Enzyme loading Neutrase® (% v/v)	0.12	
Agitation (rpm)	800	
Extraction time (min)	60	
Dependent variables	**Predicted values**	**Experimental values**
TPC (mg GAE/g DW)	118.5	122.1 ± 3.58
TFC (mg CAE/g DW)	50.0	47.3 ± 2.0
Antioxidant activity (IC_{50} μL extract/mL)	0.57	0.72 ± 0.07

Table 7 Summary of recent studies on the extraction of TPC and TFC from *R. canina* L. using various extraction methods

Extraction method	Solvent system	Extraction time (h)	SLR (% w/v)	Temperature (°C)	TPC (mg GAE/g DW)	TFC (mg/g DW)	Antioxidant activity (DPPH assay)	Ref.
Maceration	Methanol	0.03	12	4	16.61	-	95 mg gallic acid/g	[27]
	n-hexane: acetone: EtOH (2:1:1, v/v) plus 50 mg/L butylated hydroxy-toluene	0.25	-	5	2.98	1.45*	6.84 µmol/100 g	[28]
	MeOH:H_2O (60:40, v/v)	-	-	5	2.15	0.02*	94.53% radical scavenging activity	[29]
	EtOH:H_2O (40:60, v/v)	0.83	50	25	21.61	1.8***	188–397 µmol Trolox	[30]
Automatic solvent extraction	80% ethanol	1.32	1:80	-	53.62	224.4*	27.23 Mg TEAC/g	[31]
UAE and γ-valerolactone (GVL)	70:30 (v/v) EtOH/GVL	1	1:20	50	9.67	-	50 µmol TEAC/g	[32]
UAE	EtOH:H_2O (40:60, v/v)	1.35	-	25	47.23	-	-	[11]
	EtOH:H_2O (70:30, v/v)	0.50	-	50	24.00	1.4**	29 mg Trolox/g	[33]
UAEE	0.6 U/mL pectinase, 0.3 U/mL cellulase, 0.3 U/mL hemicellulase (2:1:1, v/v) in phosphate buffer pH 5.6	0.83	5	50	32.64	-	-	[15]
SFE	Supercritical CO_2	0.5	-	25	5.12	1.95*	-	[34]
EAE	Pectinex Ultra Color® 0.59%, Viscoferm® 0.51% (v/v)	1.62	6	50	123.22	49.13	0.98 µL extract/mL	[17]
	Cellic®CTec3 HS 0.1%, Pectinex Ultra Color® 0.1%, Viscoferm®0.21%, Neutrase® 0.12% (v/v)	1	6	50	122.1	47.3	0.72 µL extract/mL	Present study

* CAE: Catechin equivalents

** QE: Quercetin equivalents

*** RE: Rutin equivalents

material and matrix composition. The application of maceration with methanol:water (60:40, v/v) produced TFC values up to 10.2 mg CAE/g DW [29]. On the contrary, the replacement of the previous system with a mixture of n-hexane, acetone, and ethanol led to substantially lower TFC yields (1.5 mg CAE/g DW) [28]. Comparable low values have been observed using supercritical CO_2 extraction [34], underscoring the strong influence of solvent polarity, extraction mechanism, and matrix accessibility on flavonoid recovery.

Reported antioxidant activities of *Rosa canina* L. extracts vary widely, reflecting differences in plant material, extraction conditions, and analytical methods. It should be noted that antioxidant activity values are often expressed in different units (e.g., mg Trolox/g, mg gallic acid/g, µmol Trolox/g), making direct numerical comparison across studies challenging; nevertheless, these results provide meaningful context within the existing literature. Moldovan et al. [33] reported DPPH radical-scavenging activity corresponding to 29 mg Trolox/g DW of lyophilized extract, whereas Kayahan et al. [27] observed considerably higher activity, reaching ~ 95 mg gallic acid/g DW. Liaudanskas et al. [30] examined various *Rosa* species and cultivars and found

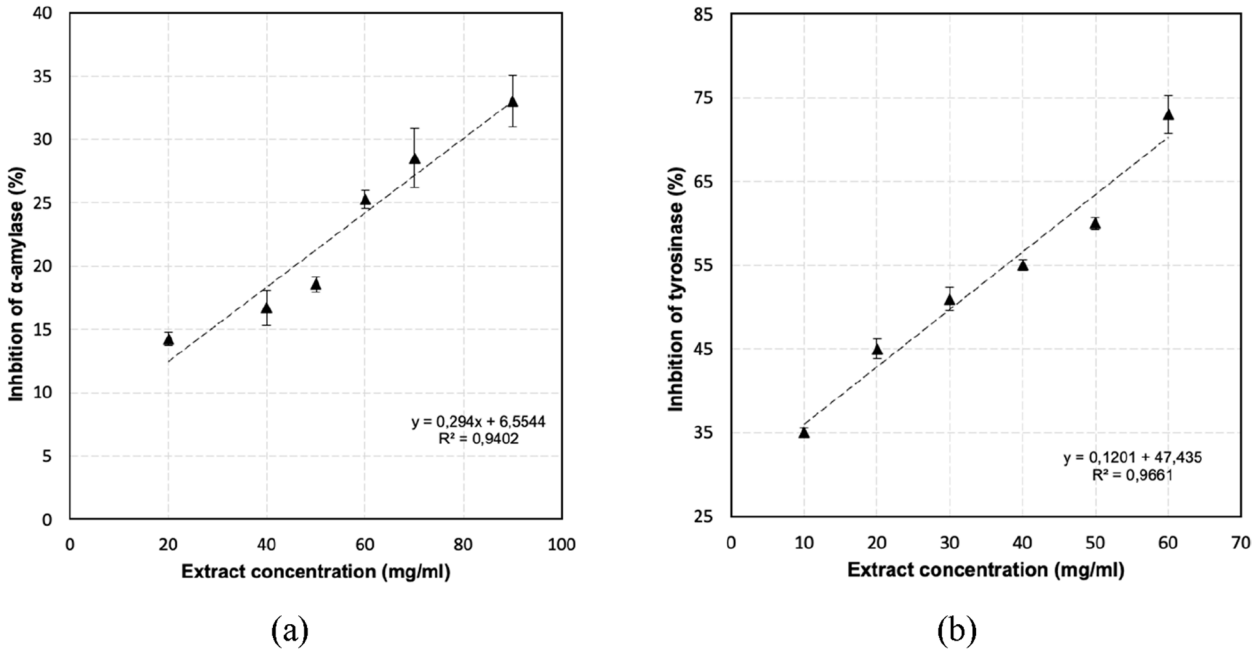


Fig. 6 Inhibitory activity of the optimum extract against **a** α-amylase and **b** tyrosinase at various concentrations. Results are expressed as percentage inhibition (%). The dashed line represents the data fitted to a linear trendline. The data are expressed as mean values ± SD

substantial variability, with antioxidant capacity ranging from 188 to 397 µmol Trolox/g. Notably, *Rosa canina* fruit extract has also been incorporated as a natural antioxidant in mayonnaise, where its antioxidant capacity was evaluated using multiple assays, yielding values of 12.3 µmol/100 g (ABTS), 6.84 (DPPH), 52.04 (FRAP), and 15,425 (CUPRAC), underscoring its functional potential in various areas [28].

Taken together, these findings demonstrate that the extraction approach developed in the present study achieves bioactive compounds yields that not only exceed many reported conventional and green extraction methods but also do so with significantly short processing times and greater process efficiency.

Biological activities of the optimum extract

Antidiabetic activity

Impaired carbohydrate metabolism and elevated blood glucose levels characterize a chronic metabolic disease, diabetes mellitus, often associated with oxidative stress and enzyme dysfunction. The inhibition of carbohydrate-hydrolyzing enzymes, such as α-amylase, delays glucose absorption by slowing the breakdown of starch into simple sugars [35–38]. The optimum extract exhibited weak inhibition of α-amylase activity, thereby weak antidiabetic activity, compared to the positive control acarbose (1 mg/ml, 100% inhibition), with an IC_{50} of 147.77 ± 4.44 mg/mL (Fig. 6a). Although EAE increased total phenolic and flavonoid yields, the extract showed only weak α-amylase inhibition. This likely reflects factors beyond phenolic concentration, including structural changes to phenolics during enzymatic hydrolysis, dilution or interference from co-extracted polysaccharides, and an extract composition enriched in phenolic subclasses with inherently low inhibitory activity. Together, these effects reduce the availability and effectiveness of bioactive compounds, explaining the limited enzyme inhibition observed [39, 40]. Future investigations should explore the factors underlying this reduced activity to better understand the differences observed.

Antiaging activity

The key enzyme involved in the biosynthesis of melanin, a protective polymer that shields the skin from ultraviolet (UV) radiation and contributes to the synthesis of vitamin D_3, is tyrosinase. It converts the amino acid tyrosine into L-DOPA and then into dopaquinone, the first two steps of melanin biosynthesis. Melanin, the pigment produced by this process, gives skin, hair, and eyes their color and absorbs harmful UV rays. However, excessive melanin production can lead to various dermatological disorders, including hyperpigmentation, wrinkles, age spots, and even melanoma [41–43]. The optimum extract derived from BBD exhibited the highest tyrosinase

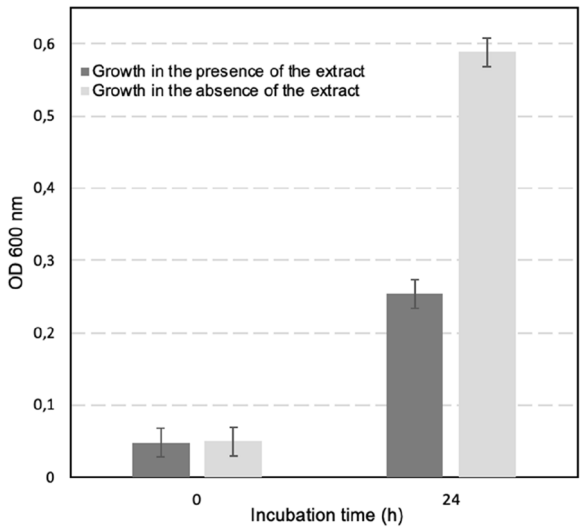


Fig. 7 Effect of *Rosa canina* L. pseudofruit optimum extract derived from BBD on *E. coli* growth. Data are expressed as mean values ± SD

inhibitory activity observed in our investigations to date, IC_{50} value of 19.16 ± 0.30 mg/mL (Fig. 6b). Although the extract exhibited lower activity than the reference compound kojic acid (1 mg/mL, 100% inhibition), it still demonstrated measurable inhibitory activity, underscoring its promise indicating its potential as a natural bioactive source for application in skin-whitening and anti-aging formulations rather than a direct substitute for the pure standard. Compared to our previous findings [17], this extract demonstrated an approximately 60% increase in anti-aging activity, which might be attributed to the enhanced extraction of bioactive compounds with tyrosinase inhibitory properties.

Numerous studies have investigated tyrosinase inhibition in diverse plant species, revealing substantial variation depending on botanical origin. Extracts from families such as Balanophoraceae and Caprifoliaceae frequently showed strong activity, whereas those from Sapotaceae, Clusiaceae, Fabaceae, Solanaceae, and Malvaceae tended to exhibit moderate inhibition. Among the most potent extracts reported are *Quercus infectoria* and *Terminalia chebula*, both with IC_{50} values of approximately 3–4 µg/mL, while many other species fell within the broader range 30–1000 µg/mL [44]. Overall, the literature highlights considerable variation tied to plant species and family.

Antibacterial activity

The antibacterial activity of the optimum extract was measured based on monitoring *E. coli* growth (OD_{600} nm) (Fig. 7) and was determined to be 52.52 ± 2.28%. Several studies have reported the antibacterial activity of *Rosa canina* L. extracts obtained through different extraction techniques; however, most express their results as Minimum Inhibitory Concentration (MIC) values, making direct comparisons challenging. In our previous works, antibacterial activity reached up to 80% when using 1.5% v/v Cellic® CTec3 HS for 360 min of extraction [16], whereas in a more recent one, we achieved 55.1% inhibition with a combination of 0.59% v/v Pectinex® Ultra Color and 0.51% v/v Viscoferm® in only 97 min [17]. In the present study, a comparable inhibition level was obtained with even shorter extraction time and lower enzyme loadings. Nevertheless, several studies have confirmed the antibacterial activity of *Rosa canina* L. pseudo-fruit extracts, particularly against *E. coli*, although the results remain inconsistent. For instance, Montazeri et al. reported moderate activity for an aqueous extract (MIC 25 mg/mL) [45], whereas a methanolic extract showed weak activity (MIC > 512 mg/mL) [46]. In contrast, other reports indicate stronger effects, with MIC values of 32 µg/mL for methanolic [47] and aqueous extracts [48], and as low as 4 mg/mL for a 70% ethanolic extract [28]. These discrepancies highlight the possibility that differences in extraction methods may influence the extraction of specific bioactive compounds responsible for antibacterial activity, an aspect that can only be clarified through detailed phytochemical profiling of the extracts, such as via LC–MS/MS [49, 50].

The enhanced extraction efficiency and biological activities observed in the present study can be attributed to the complementary and synergistic action of the four enzyme preparations on the complex plant matrix of *Rosa canina* L. pseudofruit. Plant cell walls consist of cellulose microfibrils embedded in a matrix of hemicelluloses and pectins, with structural proteins contributing to matrix cohesion and phenolic binding. The cellulolytic activity of Cellic® CTec3 HS disrupts cellulose microfibrils, while hemicellulolytic enzymes in Viscoferm® hydrolyze hemicellulose chains, enhancing structural loosening. In parallel, the pectinolytic activity of Pectinex® Ultra Color increases cell wall porosity, and the proteolytic activity of Neutrase® facilitates the release of protein-bound phenolics. The simultaneous action of these enzymes leads to synergistic matrix deconstruction, reducing mass transfer limitations and enhancing extraction efficiency.

Application of the AGREEprep tool to assess the extraction sustainability

AGREEprep was designed by Wojnowski et al. in 2022 to assess the environmental impact of processes based on the ten criteria of GSP [24]. Among the criteria is preparation location, the use of hazardous materials along with their sustainability, the energy consumption,

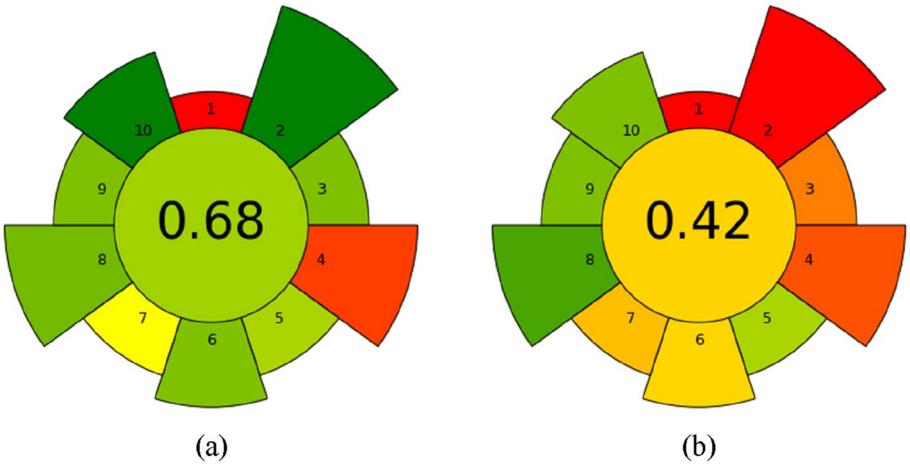


Fig. 8 Comparative AGREEprep evaluation of **a** EAE and **b** conventional ethanol:water extraction methods

the generation of waste, the sample size economy and throughput, the degree of automation, the compatibility with subsequent analytical techniques, and the operator safety. The AGREEprep output is displayed as a circular, color-coded pictogram with a central numerical score indicating the overall greenness of the sample preparation. Scores range from 0 (poor performance) to 1 (optimal performance or no sample preparation required). The surrounding circle is divided into ten segments, each representing one assessment criterion; segment length reflects its weight, while color indicates performance. This visual format enables quick comparison of overall greenness, identification of strengths and weaknesses across criteria, and clear insight into how each criterion contributes to the final result.

In this study, AGREEprep was employed to evaluate the greenness, safety, and sustainability of EAE, while the conventional ethanol:water extraction served as a comparative reference (Fig. 8). The comparison demonstrates that the EAE is greener than the ethanol:water approach, with overall scores of 0.68 and 0.42, respectively. The assessment highlighted notable advantages for EAE, particularly in terms of reduced use of hazardous materials, improved sustainability and renewability, lower waste generation, and enhanced operator's safety. These benefits arise from the exclusive use of aqueous media and biocatalysts, which eliminates flammable organic solvents and reduces chemical risks throughout the workflow. Although both methods produce comparable amounts of waste, the residues from EAE are non-hazardous and easier to manage, whereas the ethanol-containing waste of the conventional method requires stricter handling and disposal. The absence of volatile solvents in EAE also minimizes operator exposure and reduces the need for additional safety controls. Also, differences were found in sample throughput and integration and automation, mainly because the ethanol:water method requires an additional purification step to remove ethanol before analysis, increasing process complexity, basically because the conventional method needs one more purification step due to the presence of ethanol that needs to be vaporized. Overall, the AGREEprep assessment indicates that EAE represents a greener and safer alternative to ethanol:water extraction for preparing plant-based samples.

Conclusions

In this work, a multi-enzyme-assisted extraction strategy for recovering bioactive compounds from *Rosa canina* L. pseudofruit was successfully developed, optimized, and evaluated. Using a six-factor Box–Behnken Design, predictive quadratic models were established to describe the influence of enzyme loadings, agitation, and extraction time on TPC, TFC, and antioxidant activity. The optimum extract yielded significantly enhanced TPC, TFC, and antioxidant capacity compared to conventional ethanol:water extraction, along with promising biological activities. Sustainability assessment through AGREEprep further confirmed the environmental advantages of the enzymatic approach. Overall, this study demonstrates that multi-EAE represents a fast, efficient, and environmentally responsible method for the valorization of *Rosa canina* L. pseudofruit. The integration of statistical optimization, predictive modeling, and green assessment tools strengthens the case for adopting enzymatic technologies in the sustainable production of bioactive plant extracts for cosmeceuticals and nutraceutical industrial applications.

Abbreviations

EAE	Enzyme-assisted extraction
BBD	Box–Behnken Design
TPC	Total phenolic content
TFC	Total flavonoid content
GAE	Gallic acid equivalents
DW	Dry weight
CAE	Catechin equivalents
RSM	Response surface methodology
GAC	Green analytical chemistry
GSP	Green sample preparation
ANOVA	Analysis of variance
SD	Standard deviation
MIC	Minimum inhibitory concentration

Acknowledgements
The authors would like to thank Novozymes A/S, Denmark for generously providing the enzyme preparation used in the present study.

Authors' contributions
DM, AT, and AD conceptualized and supervised the research process, acquired funding, and reviewed the final draft. ZL wrote and edited the manuscript draft, prepared data visualizations, data collection and interpretation. GT carried out experimental work. TL and GS carried out software. All authors read and approved of the final manuscript.

Funding
This work was co-financed by the European Regional Development Fund of the European Union and Greek national funds through the Operational Program "Competitiveness, Entrepreneurship, and Innovation" under the call RESEARCH-CREATE-INNOVATE (grant number: T2EDK-02333, MIS 5131416).

Data availability
All data generated or analyzed during this study are included in the manuscript and supplementary information files to this article.

Declarations

Ethics approval and consent to participate
Not applicable.

Consent for publication
Not applicable.

Competing interests
The authors declare no competing interests.

Author details
[1]Biotechnology Laboratory, School of Chemical Engineering, National Technical University of Athens, 9 Iroon Polytechniou Str, Zografou Campus, Athens 15780, Greece. [2]Products and Operations Quality Control Laboratory, School of Chemical Engineering, National Technical University of Athens, 9 Iroon Polytechniou Str, Zografou Campus, Athens 15780, Greece. [3]Laboratory of Organic Chemistry, School of Chemical Engineering, National Technical University of Athens, 9 Iroon Polytechniou Str, Zografou Campus, Athens 15780, Greece. [4]Korres S.A.—Natural Products, 57th Km Athens-Lamia Road, Oinofyta Viotia 32011, Greece.

Received: 22 December 2025 Accepted: 18 February 2026
Published online: 06 April 2026

References

1. Shubayr N. Phytochemicals properties of herbal extracts for ultraviolet protection and skin health: a narrative review. J Radiat Res Appl Sci. 2023;16:100729. https://doi.org/10.1016/J.JRRAS.2023.100729.
2. Putra NR, Yustisia Y, Heryanto RB, Asmaliyah A, Miswarti M, Rizkiyah DN, et al. Advancements and challenges in green extraction techniques for Indonesian natural products: a review. S Afr J Chem Eng. 2023;46:88–98. https://doi.org/10.1016/J.SAJCE.2023.08.002.
3. Michalak M. Plant extracts as skin care and therapeutic agents. Int J Mol Sci. 2023;24:15444. https://doi.org/10.3390/IJMS242015444.
4. Puri M, Sharma D, Barrow CJ. Enzyme-assisted extraction of bioactives from plants. Trends Biotechnol. 2012;30:37–44. https://doi.org/10.1016/j.tibtech.2011.06.014.
5. Streimikyte P, Viskelis P, Viskelis J. Enzymes-assisted extraction of plants for sustainable and functional applications. Int J Mol Sci. 2022;23. https://doi.org/10.3390/ijms23042359.
6. Nadar SS, Rao P, Rathod VK. Enzyme assisted extraction of biomolecules as an approach to novel extraction technology: a review. Food Res Int. 2018;108:309–30. https://doi.org/10.1016/j.foodres.2018.03.006.
7. Hammed AM, Jaswir I, Amid A, Alam Z, Asiyanbi-H TT, Ramli N. Enzymatic hydrolysis of plants and algae for extraction of bioactive compounds. Food Rev Int. 2013;29:352–70. https://doi.org/10.1080/87559129.2013.818012.
8. Gligor O, Mocan A, Moldovan C, Locatelli M, Crișan G, Ferreira ICFR. Enzyme-assisted extractions of polyphenols – a comprehensive review. Trends Food Sci Technol. 2019;88:302–15. https://doi.org/10.1016/j.tifs.2019.03.029.
9. Bastos KVLdaS, de Souza AB, Tomé AC, Souza FdeM. New strategies for the extraction of antioxidants from fruits and their by-products: a systematic review. Plants. 2025;14:755. https://doi.org/10.3390/PLANTS14050755.
10. Box GEP, Behnken DW. Some new three level designs for the study of quantitative variables. Technometrics. 1960;2:455–75. https://doi.org/10.1080/00401706.1960.10489912.
11. Ilbay Z, Şahin S, Kirbaşlar Şİ. Optimisation of ultrasound-assisted extraction of rosehip (*Rosa canina* L.) with response surface methodology. J Sci Food Agric. 2013;93:2804–9. https://doi.org/10.1002/jsfa.6104.
12. Orhan N, Aslan M, Hoşbaş S, Deliorman Orhan D. Antidiabetic effect and antioxidant potential of *Rosa canina* fruits. Pharmacogn Mag. 2009;5:309–15. https://doi.org/10.4103/0973-1296.58151.
13. Fattahi A, Niyazi F, Shahbazi B, Farzaei MH, Bahrami G. Antidiabetic mechanisms of *Rosa canina* fruits: an in vitro evaluation. J Evid Based Complement Altern Med. 2017;22:127–33. https://doi.org/10.1177/2156587216655263.
14. Bozhuyuk MR, Ercisli S, Karatas N, Ekiert H, Elansary HO, Szopa A. Morphological and biochemical diversity in fruits of unsprayed Rosa canina and Rosa dumalis ecotypes found in different agroecological conditions. Sustainability. 2021;13. https://doi.org/10.3390/su13148060.
15. Nicolescu A, Babotă M, Zhang L, Bunea CI, Gavrilaș L, Vodnar DC, et al. Optimized ultrasound-assisted enzymatic extraction of phenolic compounds from Rosa canina L. pseudo-fruits (rosehip) and their biological activity. Antioxidants. 2022;11. https://doi.org/10.3390/antiox11061123.
16. Lemoni Z, Kalantzi S, Lymperopoulou T, Tzani A, Stavropoulos G, Detsi A, et al. Kinetic modeling and biological activities of Rosa canina L. pseudo-fruit extracts obtained via enzyme-assisted extraction. antioxidants. 2025;14. https://doi.org/10.3390/antiox14050558.
17. Lemoni Z, Kalantzi S, Lymperopoulou T, Tzani A, Stavropoulos G, Detsi A, et al. Optimization of bioactive compounds extraction from Rosa canina L. pseudofruit through the action of two hydrolytic enzyme preparations. J Chem Technol Biotechnol. 2025. https://doi.org/10.1002/jctb.70075.
18. Cannavacciuolo C, Pagliari S, Celano R, Campone L, Rastrelli L. Critical analysis of green extraction techniques used for botanicals: trends, priorities, and optimization strategies-a review. TrAC Trends Anal Chem. 2024;173. https://doi.org/10.1016/j.trac.2024.117627.
19. Kowtharapu LP, Katari NK, Muchakayala SK, Marisetti VM. Green metric tools for analytical methods assessment critical review, case studies and crucify. TrAC Trends Anal Chem. 2023;166. https://doi.org/10.1016/j.trac.2023.117196.
20. Yin L, Yu L, Guo Y, Wang C, Ge Y, Zheng X, et al. Green analytical chemistry metrics for evaluating the greenness of analytical procedures. J Pharm Anal. 2024;14. https://doi.org/10.1016/j.jpha.2024.101013.
21. Nowak PM, Wietecha-Posłuszny R, Pawliszyn J. White analytical chemistry: an approach to reconcile the principles of Green Analytical Chemistry and functionality. TrAC Trends Anal Chem. 2021;138:116223. https://doi.org/10.1016/J.TRAC.2021.116223.
22. Anastas PT, Warner JC. Green chemistry: theory and practice. 2000. https://doi.org/10.1093/OSO/9780198506980.001.0001.
23. Pena-Pereira F, Tobiszewski M, Wojnowski W, Psillakis E. A tutorial on AGREEprep an analytical greenness metric for sample preparation. Adv Sample Prep. 2022;3:100025. https://doi.org/10.1016/J.SAMPRE.2022.100025.

24. Wojnowski W, Tobiszewski M, Pena-Pereira F, Psillakis E. AGREEprep – analytical greenness metric for sample preparation. TrAC Trends Anal Chem. 2022;149. https://doi.org/10.1016/j.trac.2022.116553.
25. Passerine BFG, Breitkreitz MC. Important aspects of the design of experiments and data treatment in the analytical quality by design framework for chromatographic method development. Molecules. 2024;29:6057. https://doi.org/10.3390/molecules29246057.
26. Derringer G, Suich R. Simultaneous optimization of several response variables. J Qual Technol. 1980;12:214–9. https://doi.org/10.1080/00224065.1980.11980968.
27. Kayahan S, Ozdemir Y, Gulbag F. Functional compounds and antioxidant activity of rosa species grown in Turkey. Erwerbs-obstbau. 2023;65:1079–86. https://doi.org/10.1007/s10341-022-00688-5.
28. Miljković VM, Nikolić L, Mrmošanin J, Gajić I, Mihajilov-Krstev T, Zvezdanović J, et al. Chemical profile and antioxidant and antimicrobial activity of Rosa canina L. dried fruit commercially available in Serbia. Int J Mol Sci. 2024;25. https://doi.org/10.3390/ijms25052518.
29. Maloupa E, Karapatzak E, Ganopoulos I, Karydas A, Papanastasi K, Kyrkas D, et al. Molecular authentication, phytochemical evaluation and asexual propagation of wild-growing Rosa canina l. (rosaceae) genotypes of northern greece for sustainable exploitation. Plants. 2021;10. https://doi.org/10.3390/plants10122634.
30. Liaudanskas M, Noreikienė I, Zymonė K, Juodytė R, Žvikas V, Janulis V. Composition and antioxidant activity of phenolic compounds in fruit of the genus Rosa L. antioxidants. 2021;10. https://doi.org/10.3390/antiox10040545.
31. Bozkurt RN, Şahin S. Green Synthesis of zinc oxide nanoparticles including rosehip (Rosa canina L.) seed extract: evaluation of its characterization and bioactivity properties. Chem Biodivers. 2025;22. https://doi.org/10.1002/cbdv.202402724.
32. Kaczkowska H, Pestriakova M, Wółkiewicz J, Krakowska-Sieprawska A, Fijałkowski P, Rafiński Z, et al. Sustainable Extraction of bioactive phenolics from rose hips for functional food applications: evaluation of green solvents and extraction techniques. Foods. 2025;14. https://doi.org/10.3390/foods14142448.
33. Moldovan C, Babota M, Mocan A, Menghini L, Cesa S, Gavan A, et al. Optimization of the drying process of autumn fruits rich in antioxidants: a study focusing on rosehip (: Rosa canina L.) and sea buckthorn (Elaeagnus rhamnoides (L.) A. Nelson) and their bioactive properties. Food Funct. 2021;12:3939–53. https://doi.org/10.1039/d0fo02783a.
34. Mihalcea L, Păcularu-Burada B, Milea Ștefania A, Aprodu I, Condurache (Lazăr) NN, Cucolea EI, et al. CO2 supercritical extraction and microencapsulation of oleoresins from rosehip fruits for getting powders with multiple applications. Curr Res Food Sci. 2023;6. https://doi.org/10.1016/j.crfs.2023.100449.
35. Kalinovskii AP, Sintsova O V., Gladkikh IN, Leychenko E V. Natural inhibitors of mammalian α-amylases as promising drugs for the treatment of metabolic diseases. Int J Mol Sci. 2023;24. https://doi.org/10.3390/ijms242216514.
36. Safamansouri H, Nikan M, Amin G, Sarkhail P, Gohari AR, Kurepaz-Mahmoodabadi M, et al. α-Amylase inhibitory activity of some traditionally used medicinal species of Labiatae. J Diabetes Metab Disord. 2014;13:114. https://doi.org/10.1186/S40200-014-0114-1.
37. Oluwagunwa OA, Alashi AM, Aluko RE. Inhibition of the in vitro activities of α-amylase and pancreatic lipase by aqueous extracts of *Amaranthus viridis*, *Solanum macrocarpon* and *Telfairia occidentalis* leaves. Front Nutr. 2021;8:772903. https://doi.org/10.3389/fnut.2021.772903.
38. Yan LJ. Pathogenesis of chronic hyperglycemia: from reductive stress to oxidative stress. J Diabetes Res. 2014;2014:137919. https://doi.org/10.1155/2014/137919.
39. El-Nashar HAS, Gamal El-Din MI, Hritcu L, Eldahshan OA. Insights on the inhibitory power of flavonoids on tyrosinase activity: a survey from 2016 to 2021. Molecules. 2021;26. https://doi.org/10.3390/molecules26247546.
40. Xiao J, Ni X, Kai G, Chen X. A review on structure-activity relationship of dietary polyphenols inhibiting α-amylase. Crit Rev Food Sci Nutr. 2013;53:497–506. https://doi.org/10.1080/10408398.2010.548108.
41. Namiecińska E, Jaszczak J, Hikisz P, Daśko M, Woźniczka M, Budzisz E. Evaluation of tyrosinase inhibitory activity of carbathioamidopyrazoles and their potential application in cosmetic products and melanoma treatment. Int J Mol Sci. 2025;26. https://doi.org/10.3390/ijms26083882.
42. Di Petrillo A, González-Paramás AM, Era B, Medda R, Pintus F, Santos-Buelga C, et al. Tyrosinase inhibition and antioxidant properties of *Asphodelus microcarpus* extracts. BMC Complement Altern Med. 2016;16:453. https://doi.org/10.1186/S12906-016-1442-0.
43. Hassan M, Shahzadi S, Kloczkowski A. Tyrosinase inhibitors naturally present in plants and synthetic modifications of these natural products as anti-melanogenic agents: a review. Molecules. 2023;28:378. https://doi.org/10.3390/MOLECULES28010378.
44. Ekanayaka EMTA, De Silva WS. A review on tyrosinase inhibition potential of plant extracts for skin whitening. Vavuniya J Sci. 2023;2:1–7. https://doi.org/10.4038/vjs.v2i1.16.
45. Montazeri N, Baher E, Mirzajani F, Barami Z, Yousefian S. Phytochemical contents and biological activities of *Rosa canina* fruit from Iran. J Med Plants Res. 2011;5:4584–9. https://doi.org/10.1016/j.lwt.2021.112716.
46. Oyedemi SO, Oyedemi BO, Prieto JM, Coopoosamy RM, Stapleton P, Gibbons S. In vitro assessment of antibiotic-resistance reversal of a methanol extract from *Rosa canina* L. S Afr J Bot. 2016;105:337–42. https://doi.org/10.1016/j.sajb.2016.03.013.
47. Rovná K, Ivanišová E, Žiarovská J, Ferus P, Terentjeva M, Kowalczewski PŁ, et al. Characterization of rosa canina fruits collected in urban areas of Slovakia. Genome size, IPBS profiles and antioxidant and antimicrobial activities. Molecules. 2020;25. https://doi.org/10.3390/molecules25081888.
48. Polumackanycz M, Kaszuba M, Konopacka A, Marzec-Wróblewska U, Wesolowski M, Waleron K, et al. Phenolic composition and biological properties of wild and commercial dog rose fruits and leaves. Molecules. 2020;25. https://doi.org/10.3390/MOLECULES25225272.
49. Zhang QW, Lin LG, Ye WC. Techniques for extraction and isolation of natural products: a comprehensive review. Chin Med. 2018;13. https://doi.org/10.1186/s13020-018-0177-x.
50. Sasidharan S, Chen Y, Saravanan D, Sundram KM, Latha LY. Extraction, isolation andcharacterization of bioactive compounds from plants' extracts. Afr J Tradit Complement Altern Med. 2011;8:1–10.

Publisher's Note

Springer Nature remains neutral with regard to jurisdictional claims in published maps and institutional affiliations.